ซิงก์ออกไซด์/แกรฟีนนาโนคอมพอสิตเพื่อเป็นขั้วไฟฟ้าชนิดใหม่สำหรับตัวรับรู้ทางเคมีไฟฟ้า

นายพงศกร ก้องสิทธิกุล

วิทยานิพนธ์นี้เป็นส่วนหนึ่งของการศึกษาตามหลักสูตรปริญญาวิทยาศาสตรมหาบัณฑิต
สาขาวิชาปิโตรเคมีและวิทยาศาสตร์พอลิเมอร์
คณะวิทยาศาสตร์ จุฬาลงกรณ์มหาวิทยาลัย
ปีการศึกษา 2559

ZINC OXIDE/GRAPHENE NANOCOMPOSITES AS NOVEL ELECTRODE FOR ELECTROCHEMICAL SENSOR

Mr. Pongsakorn Kongsittikul

A Thesis Submitted in Partial Fulfillment of the Requirements
for the Degree of Master of Science Program in Petrochemistry and Polymer Science
Faculty of Science
Chulalongkorn University
Academic Year 2016

Thesis Title	ZINC OXIDE/GRAPHENE NANOCOMPOSITES AS NOVEL ELECTRODE FOR ELECTROCHEMICAL SENSOR
By	Mr. Pongsakorn Kongsittikul
Field of Study	Petrochemistry and Polymer Science
Thesis Advisor	Professor Orawon Chailapakul, Ph.D.
Thesis Co-Advisor	Nadnudda Rodthongkum, Ph.D.

Accepted by the Faculty of Science, Chulalongkorn University in Partial Fulfillment of the Requirements for the Master's Degree

.....Dean of the Faculty of Science
(Associate Professor Polkit Sangvanich, Ph.D.)

THESIS COMMITTEE

.....Chairman
(Professor Pattarapan Prasassarakich, Ph.D.)

.....Thesis Advisor
(Professor Orawon Chailapakul, Ph.D.)

.....Thesis Co-Advisor
(Nadnudda Rodthongkum, Ph.D.)

.....Examiner
(Associate Professor Prasert Reubroycharoen, Ph.D.)

.....External Examiner
(Associate Professor Weena Siangproh, Ph.D.)

พงศกร ก้องสิทธิกุล : ซิงก์ออกไซด์/แกรฟีนนาโนคอมพอสิตเพื่อเป็นขั้วไฟฟ้าชนิดใหม่สำหรับตัวรับรู้ทางเคมีไฟฟ้า (ZINC OXIDE/GRAPHENE NANOCOMPOSITES AS NOVEL ELECTRODE FOR ELECTROCHEMICAL SENSOR) อ.ที่ปรึกษาวิทยานิพนธ์หลัก: ศ. ดร.อรวรรณ ชัยลภากุล, อ.ที่ปรึกษาวิทยานิพนธ์ร่วม: ดร.นาฏนัดดา รอดทองคำ, 59 หน้า.

ซิงก์ออกไซด์ชนิดแท่งอนุภาคเล็กระดับนาโนถูกเตรียมผ่านกระบวนการสลายตัวทางความร้อนโดยใช้ซิงก์แอซิเทตไดไฮเดรทเป็นสารตั้งต้น จากนั้นซิงก์ออกไซด์ชนิดแท่งอนุภาคเล็กระดับนาโนจะถูกนำไปใช้ในการสังเคราะห์ซิงก์ออกไซด์/แกรฟีนนาโนคอมพอสิตด้วยเทคนิคการตกตะกอนร่วมของสารแขวนลอยภายใต้อุณหภูมิห้อง หลังจากนั้นซิงก์ออกไซด์/แกรฟีนนาโนคอมพอสิตที่สังเคราะห์ได้จะถูกนำมาใช้ในการดัดแปรพื้นที่ผิวของตัวรับรู้ทางเคมีไฟฟ้าสำหรับการตรวจวัดแคดเมียมและตะกั่วสองชนิดพร้อมกัน จากผลการศึกษาสัณฐานวิทยาของซิงก์ออกไซด์และซิงก์ออกไซด์/แกรฟีนนาโนคอมพอสิตด้วยกล้องจุลทรรศน์อิเล็กตรอนชนิดส่องผ่านและส่องกราดพบว่า ซิงก์ออกไซด์ชนิดแท่งอนุภาคเล็กระดับนาโนมีขนาดเส้นผ่านศูนย์กลางของอนุภาคเฉลี่ยเท่ากับ 93±21 นาโนเมตร กระจายตัวอย่างสม่ำเสมอบนแผ่นแกรฟีน ยิ่งไปกว่านั้น ปัจจัยที่ส่งผลต่อความไวในการตรวจวัดแคดเมียมและตะกั่วของระบบนี้ถูกนำมาศึกษาและหาสภาวะที่เหมาะสมที่สุดด้วยเทคนิคแอโนดิกสทริปปิงโวลแทมเมตรี โดยภายใต้สภาวะที่เหมาะสม ระบบการตรวจวัดนี้มีขีดจำกัดในการตรวจวัดแคดเมียมและตะกั่วเป็น 0.6 และ 0.8 ไมโครกรัมต่อลิตร ตามลำดับ และสามารถวัดได้ต่ำในช่วง 10 ถึง 200 ไมโครกรัมต่อลิตร นอกจากนี้ระบบที่ใช้ในการตรวจวัดนี้ยังถูกนำไปประยุกต์ใช้สำหรับการตรวจวัดแคดเมียมและตะกั่วในน้ำเสียจากโรงงานอุตสาหกรรม ซึ่งจากผลการดทดสอบพบว่าเทคนิคที่พัฒนาในงานวิจัยนี้ให้ผลที่ดีและสอดคล้องกับเทคนิคมาตรฐานอินดักทีฟลีคัพเพิลพลาสมาออพติคอลอิมิสชันสเปกโทรเมตรี

สาขาวิชา ปิโตรเคมีและวิทยาศาสตร์พอลิเมอร์ ลายมือชื่อนิสิต .....

ปีการศึกษา 2559 ลายมือชื่อ อ.ที่ปรึกษาหลัก .....

ลายมือชื่อ อ.ที่ปรึกษาร่วม .....

5672022623 : MAJOR PETROCHEMISTRY AND POLYMER SCIENCE
KEYWORDS: ZINC OXIDE NANORODS, GRAPHENE, ELECTROCHEMICAL SENSOR, CADMIUM, LEAD

PONGSAKORN KONGSITTIKUL: ZINC OXIDE/GRAPHENE NANOCOMPOSITES AS NOVEL ELECTRODE FOR ELECTROCHEMICAL SENSOR. ADVISOR: PROF. ORAWON CHAILAPAKUL, Ph.D., CO-ADVISOR: NADNUDDA RODTHONGKUM, Ph.D., 59 pp.

Zinc Oxide (ZnO) nanorods were prepared using zinc acetate as a precursor via modified thermal pyrolysis method and used to synthesize ZnO/graphene (ZnO/G) nanocomposites. The as prepared nanocomposites were successfully synthesized by a facile room-temperature approach using the colloidal coagulation effect. Afterwards, ZnO/G nanocomposites were used for electrode surface modification in an electrochemical sensor for the simultaneous determination of cadmium (Cd^{2+}) and lead (Pb^{2+}). The results obtained from transmission electron microscopy and scanning electron microscopy showed that ZnO nanarods with an average diameter of 93 ± 21 nm were uniformly dispersed on G nanosheets. Moreover, the factors affecting the electrochemical sensitivity of this system for the simultaneous determination of Cd^{2+} and Pb^{2+} were optimized using square-wave anodic stripping voltammetry. Under the optimized conditions, this system provided the detection limits (S/N=3) of 0.6 and 0.8 $\mu g \cdot L^{-1}$ for Cd^{2+} and Pb^{2+}, respectively and a linear range was found to be 10-200 $\mu g \cdot L^{-1}$. Furthermore, this system provided the satisfied results for determination of Cd^{2+} and Pb^{2+} in wastewater samples compared with a standard inductively coupled plasma-optical emission spectroscopy.

Field of Study:	Petrochemistry and Polymer Science	Student's Signature .....
		Advisor's Signature .....
Academic Year:	2016	Co-Advisor's Signature .....

ACKNOWLEDGEMENTS

I would like to thank all my thesis advisor and co-advisors including Professor Dr. Orawon Chailapakul and Dr. Nadnudda Rodthongkum for their support and good advice for everything on this thesis.

I would like to thank to Dr. Jiaqian Qin for his advices and process synthesis of ZnO and ZnO/G nanocomposite.

I would like to thank to Ms. Kanokwan Saengkiettiyut for her advices about electrochemical instrument.

I am grateful to all the thesis committee members including Professor Dr. Pattarapan Prasassarakich, Associate Professor Dr. Prasert Reubroycharoen and Associate Professor Dr. Weena Siangproh for their comments and suggestion.

I would like to appreciate the financial supports from the National Nanotechnology Center (NANOTEC), NSTDA, Ministry of Science and Technology, Thailand and Ratchadaphisek Sompoch, Endowmetn Fund, Chulalongkorn University and the Asahi Glass Foundation.

I am also thankful for all supports, advices and warm friendship from my research group.

Finally, I would like to thank to my lovely family for their love and encouragement throughout my life.

CONTENTS

Page

Page

Page

Page

LIST OF TABLES

Page

LIST OF FIGURES

Page

CHAPTER I
INTRODUCTION

1.1 Introduction

Electrochemical technique has been widely used in various sensor applications, such as medical diagnosis [1], food inspection [2] and environmental monitoring [3, 4] because of its simplicity, low operating cost and high sensitivity. The conventional electrochemical cell consists of three electrodes including reference electrode, counter electrode and working electrode. Later, the electrode was designed to be a portable size for field based site analysis, which is called screen-printed carbon electrode or SPCE [5]. Moreover, one of the most important advantages of SPCE compared with conventional electrode is small amount of sample requirement. However, the surface area of working electrode is automatically limited by its size, leading to low sensitivity. Therefore, the modification of working electrode surface is greatly required in order to improve both sensitivity and analytical performances. To increase the surface area of working electrode, the working electrode surface is usually modified by various nanoparticles such as conductive polymer [1, 5], metallic nanoparticles [6], metal oxide nanoparticles [7] and carbon-based nanomaterials [8]. In the recent years, graphene (G), a single layer of graphite, is one of the promising materials because of its unique properties, such as high specific surface area, high electron transfer and high conductivity [9]. According to these properties, G has been applied in several applications including, energy storage [10], drug delivery [11] as well as electrochemical sensor [12, 13]. However, the self-agglomeration of G is a crucial problem decreasing its important properties [14]. To solve this problem, other nanomaterials such as metal oxides were used to form nanocomposite with G [7]. Among metal oxide based materials, ZnO has received much attentions in the electrochemical applications due to its outstanding properties, such as high electron mobility, high stability, high electrocatalytic activity biocompatibility and high specific surface [15-17]. Moreover, the morphology of ZnO is varied depending on the synthesis method and raw material, such as, nanorods [18], nanowires [19], nanobelts [20],

nanotubes [21] and nanosheets [22]. From the previous work, it has been reported that, among various shapes of ZnO nanostructure, ZnO nanorods can form three dimensional (3D) structure after blending with G to obtain large surface area [23]. Therefore, the ZnO/G nanocomposite has been widely used in various applications, such as photocatalyst [24, 25] and electrochemical sensor [26]. Recently, there are some previous reports about using the ZnO/G nanocomposite to modify the working electrode surface in electrochemical sensor for detection of glucose [27] and simultaneous detection of ascorbic acid, dopamine and uric acid [28]. Moreover, this material has a high potential to use for the detection of other analytes.

Toxic heavy metals, such as cadmium (Cd^{2+}) and lead (Pb^{2+}), are the important analytes that can cause serious problem for environment and human health even at their low levels. These heavy metals are non-biodegradable and very difficult to be eliminated. Thus, the natural resources can be easily contaminated by these toxic heavy metals. Besides, the accumulation of heavy metals in human body can cause several diseases such as kidney, liver and bone [29, 30]. In general, there are several analytical methods have been used for heavy metal detection, such as atomic absorption spectroscopy (AAS) [31], inductively coupled plasma-mass spectrometry (ICP-MS) [32] and inductively couples plasma optical emission spectrometry (ICP-OES) [33]. Although these traditional methods provide the high sensitivity and selectivity, they require specialized operator, high operating cost and long analysis time [34]. Therefore, the electrochemistry has become an alternative choice due to its portability, simplicity, low cost and also rapid analysis [35]. So, in this study, we propose to develop a novel electrochemical sensor based on ZnO/G modified electrode for the determination of $Cd^{2+}$and Pb^{2+}. Finally, our system was applied for simultaneous detection of Cd^{2+} and Pb^{2+} in wastewater samples and the results are corresponded well with the results obtained from a standard ICP-OES method.

1.2 Objective

- To synthesize ZnO/G nanocomposite for electrode surface modification.
- To modify the electrochemical sensor by using synthesized ZnO/G and apply it for simultaneous determination of Cd^{2+} and Pb^{2+}.
- To apply this system for the detection of Cd^{2+} and Pb^{2+} in wastewater samples.

1.3 Scope of the thesis

In this study, the ZnO nanorods were prepared by using zinc acetate as a precursor via thermal decomposition method and used to synthesize the ZnO/G nanocomposite by facile room-temperature approach using a colloidal coagulation effect. Then, the synthesized ZnO/G was used to modify the working electrode surface and applied for the simultaneous determination of Cd^{2+} and Pb^{2+}. Moreover, the important parameters affecting on electrochemical sensitivity of our system such as ZnO/G ratio, ZnO/G concentration, Bi^{3+} concentration and electrochemical parameters were investigated and optimized. Besides, the analytical performances of modified electrode such as, a linear range and limit of detection were evaluated. Eventually, under the optimum conditions, the ZnO/G modified electrochemical sensor was used to detect Cd^{2+} and Pb^{2+} in real wastewater samples and compared with a standard ICP-OES method.

CHAPTER II

THEORY AND LITERATURE SURVEY

In this chapter, the theory and basic principles of electrochemical analysis are introduced. The preparation of screen-printed electrode is illustrated. The surface modification of screen-printed carbon electrode by using nanomaterials (e.g. graphene, zinc oxide, zinc oxide/graphene nanocomposite) are explained. Moreover, the detection of heavy metals by using electrochemical sensor is described.

2.1 Electrochemistry and electrochemical analysis [36, 37]

Electrochemistry is defined as a branch of chemistry that investigates the phenomena resulting from combined chemical and electrical effect. The principle of electrochemistry has been extensively applied in several applications including corrosion study, fuel cell, energy storage as well as electrochemical sensor.

Electrochemical detection, one of analytical techniques can be used to study for both qualitative and quantitative analysis, has been widely used in various field such as medical diagnosis, food inspection and environment survey because this technique provides the simple process, high sensitivity and also low operating cost. In an electrochemical cell, there are three main components including three electrodes (working electrode, counter electrode and reference electrode), electrolyte and external power supply. The conventional three-electrode cell is shown in Figure 2.1. For electrochemical measurement, the electrochemical reaction is occur at the interface between the working electrode surface and electrolyte solution based on oxidation and reduction process of target analyte.

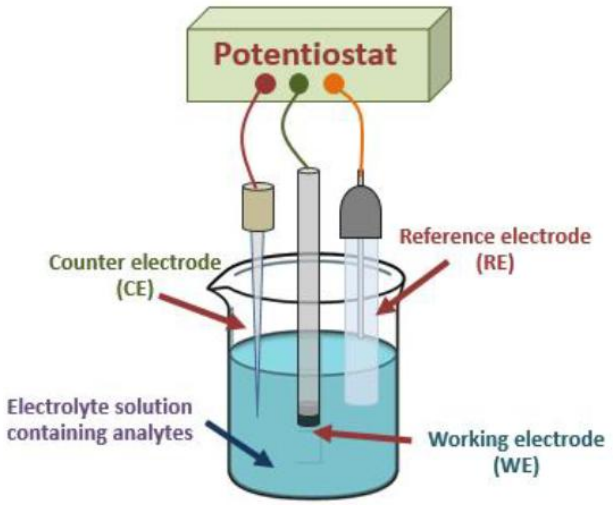

Figure 2.1 The conventional three-electrode cell.

In general, the electrochemical measurements are classified into two types, including potentiometric and potentiostatic. Potentiometric technique is a static technique (zero current) that measures the potential of a solution between two electrodes (working electrode and reference electrode). Potentiostatic technique is a dynamic technique (no zero current) that measures the current response obtained from electron-transfer reaction when the working electrode is applied by controlled potential. There are several potentiostatic methods such as voltammetry, amperometry and coulometry, have been widely used for the development of electrochemical sensor. However, in this study, we only used the voltammetric methods including cyclic voltammetry and anodic stripping voltammetry to characterize the electrochemical properties of an electrochemical sensor prepared in this study.

2.1.1 Cyclic voltammetry

Cyclic voltammetry (CV) is a basic technique has been widely used in electrochemical analysis due to its simplicity. So this technique usually used for preliminary study the electrochemical reaction of the new system. In general, this technique will be applied potential in two steps versus time as waveform which is called “triangular waveform” as seen in Figure 2.1a. The first step, the potential scan in forward direction (anodically scan) and the next step is switching the direction of scan (at E_λ) to opposite direction (cathodically scan). The output resulting from CV is called cyclic voltammogram. The graph plot between applied potential versus the

current intensity as seen in Figure 2.1b. There are two important peak obtained from cyclic voltammogram consists of cathodic peak and anodic peak that came from oxidation and reduction reaction, respectively.

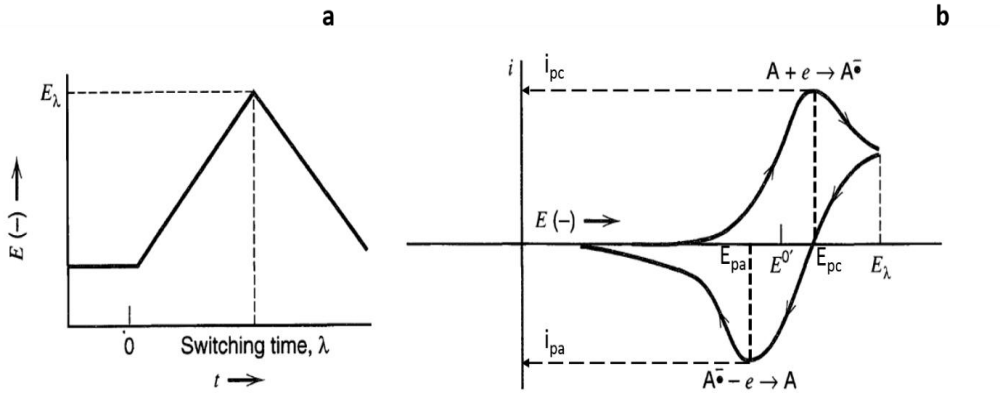

Figure 2.2 (a) Applied potential of CV (triangular waveform) and (b) cyclic voltammogram.

Moreover, there are also four values that used for electrochemical characterization including cathodic peak current (i_{pc}), anodic peak current (i_{pa}), cathodic peak potential (E_{pc}) and anodic peak potential (E_{pa}). The cathodic and anodic peak current response can be described by the highest peak current of reduction and oxidation peak, respectively. In the same way, the cathodic and anodic peak potential can be described by the location of peak appearance of reduction and oxidation peak, respectively. The calculation of peak current response for a reversible redox couple at 25°C is given by Randles-Sevcik equation:

$$i_p = (2.69 \times 10^5)\, n^{3/2} A C D_o^{\ 1/2} \mathbf{V}^{1/2}$$

where n = number of transferred electrons

A = area of electrode surface (cm^2)

C = concentration of electroactive species (mol/cm^3)

D_o = diffusion coefficient (cm^2/s)

V = scan rate (V/s)

2.1.2 Anodic stripping voltammetry

Anodic stripping voltammetry (ASV), one of electroanalytical techniques, is the most widely used for heavy metal determination in trace level, because this technique can be accumulated the metal ions on electrode surface during the deposition step (or accumulation step). Briefly, for mercury electrode, there are two steps for ASV measurement.

Firstly, the accumulation step, the deposition potential (E_d) is applied more negative than E^0 of target metals in a controlled time (deposition time; T_d). Then, all of target metal ions are reduced and accumulated as amalgams (M/Hg) on working electrode surface.

$$M^{+n} + ne^- + Hg \longrightarrow M(Hg)$$

Secondly, the stripping step, the applied potential is linearly scanned in forward direction. The amalgamated metals are reoxidized and stripped out of working electrode surface. The current response is obtained.

$$M(Hg) \longrightarrow M^{+n} + ne^- + Hg$$

Finally, the results obtained from ASV, anodic stripping voltammogram, is shown in Figure 2.3

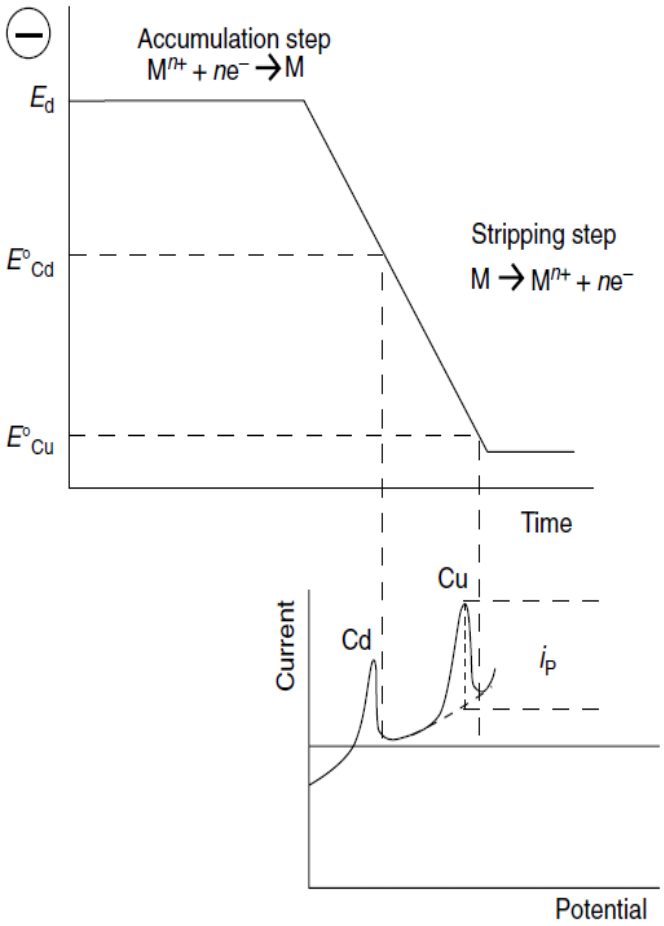

Figure 2.3 The relation of applied potential with controlled time and the output obtained from anodic stripping voltammetry (Anodic stripping voltammogram).

2.2 Screen-printed technique

Nowadays, the conventional three electrode cell has been developed and designed to be a small size which is called screen-printed electrode. The advantages of screen printed electrode are simple equipment, low preparation cost and also use small amount of sample. Moreover, the most advantage of screen printed electrode is portability. Because of this property, the screen printed electrode can be applied for field based sensor application such as medical diagnosis and environmental survey.

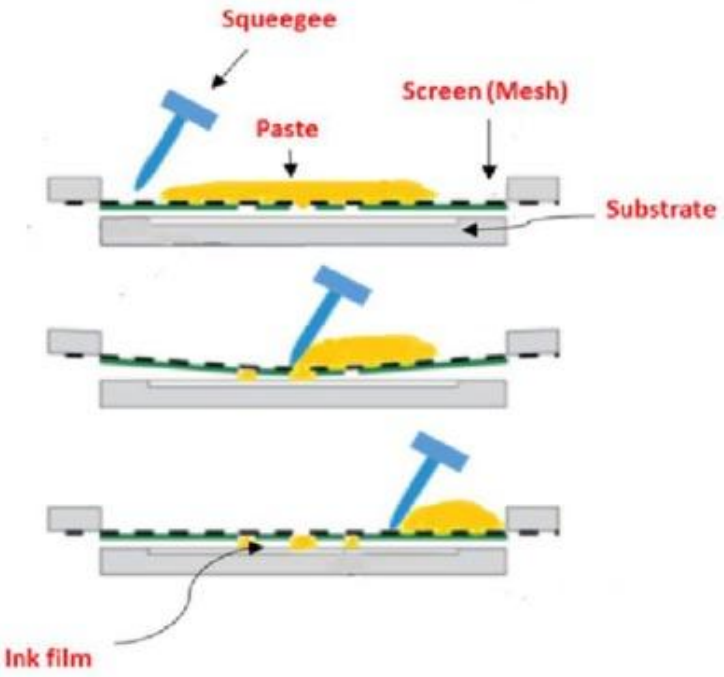

Figure 2.4 Schematic diagram of the screen printing basic process for electrodes manufacturing [38].

The fabrication of screen printed electrode can be produced by using a woven mesh supported an ink-blocking-stencil, a conductive ink, a substrate and a squeegee. The process of screen printed electrode are shown in Figure 2.4. The configuration of screen printed electrode is flexible designed depending on type of target analyte. The plastic based or paper based materials can be used as substrate. The most advantage of substrate prepared by plastic-based over the paper-based is reusability. Thus, in this study, we focused on the screen-printed carbon electrode (SPCE) using Poly (vinyl chloride) (PVC) as substrate. The SPCE configurations are shown in Figure 2.5.

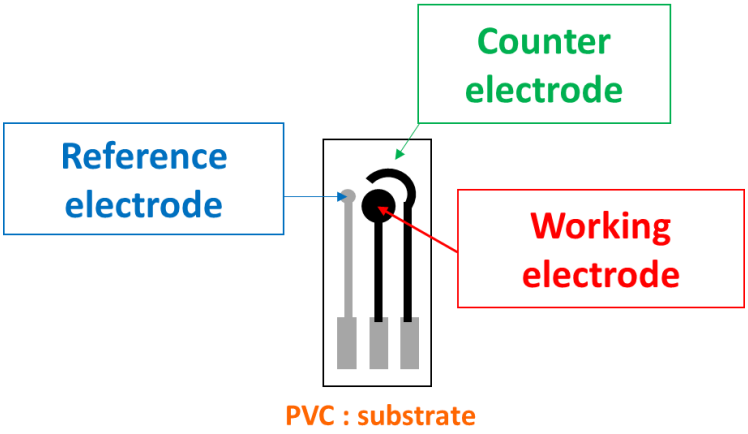

Figure 2.5 Screen-printed carbon electrode (SPCE) prepared in this study [1, 4, 5].

However, the conductive ink for screen printed electrode consists of some mineral binders or insulating polymer for increase the adhesive property with the substrate. These insulating component can inhibit the electrical conductivity of screen printed electrode cause decrease in electron transfer rate leading to low electrochemical sensitivity. Moreover, the surface area of working electrode is limited by its portable size leading to low electrochemical sensitivity. To solve these problem, the electrode surface modification is required to improve the electrochemical properties before using in the electrochemical sensor application.

2.3 Electrode surface modification

In general, the conventional sensor used in electrochemical application consists of three electrode including working electrode, counter electrode and reference electrode. Among all, the working electrode is the most important electrode because the electrochemical reaction is occurred on the surface of working electrode. So, the modification of working electrode surface area is greatly necessary. In order to increase the specific surface area of working electrode, the nanomaterials, such as carbon-based nanomaterials, metal oxides, metals and conducting polymers are extensively used for electrode surface modification. Moreover, the high specific surface area cause increase in electrochemical reactivity area leading to high electrochemical sensitivity.

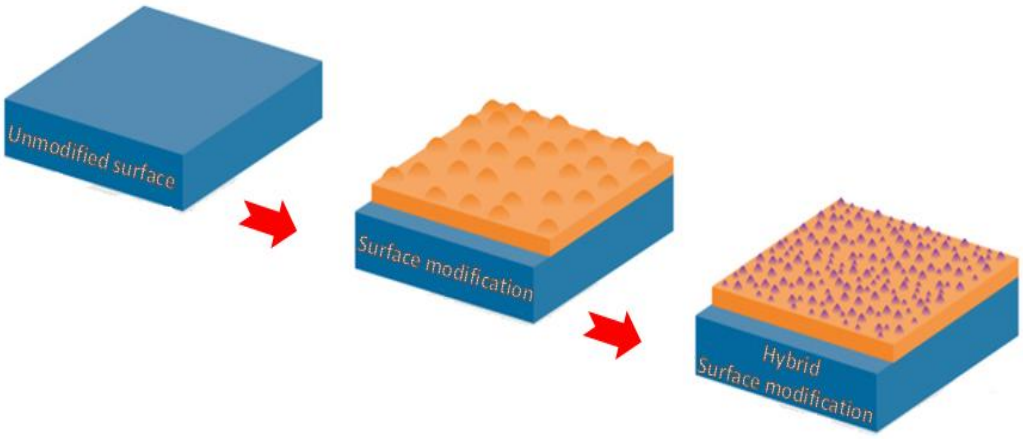

Figure 2.6 Model of surface modification by using nanomaterial and composite nanomaterial.

2.4 Nano sized materials

2.4.1 Carbon-based nanomaterials

Carbon-based nanomaterials such as single-wall carbon nanotubes, multi-wall carbon nanotubes, fullerene and graphene have been widely used to modify the working electrode surface in various electrochemical sensor due to their outstanding properties such as high conductivity, high electron mobility and high specific surface area [1, 3, 5, 39] leading to high electrochemical sensitivity and also high electron mobility of modified electrode. However, carbon nanotubes can be contaminated by metal nanoparticles during preparation step even after multi-step carbon nanotubes purification. The presence of contaminated metal nanoparticles in carbon nanotubes modified electrode can interfere the electrochemical sensitivity of target analyte leading to low accuracy and electrochemical sensitivity. In order to avoid this problem, graphene was suggested as a promising material for electrode surface modification without impurity instead of carbon nanotubes.

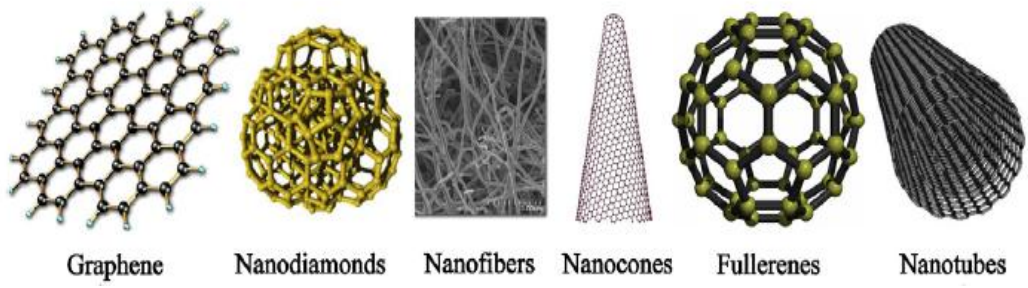

Figure 2.7 Carbon-based nanomaterials [40].

Graphene, defined as a single layer of graphite, is an allotrope of carbon in form of a two-dimensional (2D) honey-comb lattice. Graphene has become an interesting material used for electrode surface modification due to its extraordinary properties, including excellent conductivity, high electrocatalytic activity and extremely large surface area (2600 $m^2 \cdot g^{-1}$) [9-10]. Therefore, there are many reports have been used graphene for modified surface of electrochemical sensor.

Wonsawat et al. [41] developed an electrochemical sensor based on graphene modified carbon paste electrode for simultaneous detection of Cd^{2+} and Pb^{2+}. The obtained results confirmed that, the high conductivity and high surface area of graphene can enhance the electrochemical sensitivity of carbon paste electrode for the simultaneous 4 detection of Cd^{2+} and Pb^{2+}. Moreover, this developed electrode showed extremely low detection limits for both Cd^{2+} and Pb^{2+} when comparing with carbon nanotubes based modified carbon paste electrode in the previous work.

However, the self-agglomeration of graphene is a crucial problem decreasing its important properties. To solve this problem, other nanomaterials such as metal oxides were used to form nanocomposite with graphene.

2.4.2 Metal oxide

The various types of metal oxide such as tin dioxide (SnO_2), titanium dioxide (TiO_2), iron oxide (Fe_2O_3) and zinc oxide (ZnO) have been used to improve the electrochemical sensitivity in electrochemical sensor application [42-45]. Among metal oxide based nanomaterials, ZnO, is a wide band-gap semi-conductor with wurtzite structure, has received much attentions in the electrochemical application due to its

unique properties, such as high electron mobility, high electro catalytic activity, high stability, good biocompatibility and high specific surface area [15, 19]. Moreover, the uniqueness of ZnO is the variety of ZnO nanostructures. The nanostructure of ZnO is varied depending on the synthesis method and the raw materials such as, nanotubes, nanowires, nanoparticles, nanosheets, nanoflowers and nanorods etc.

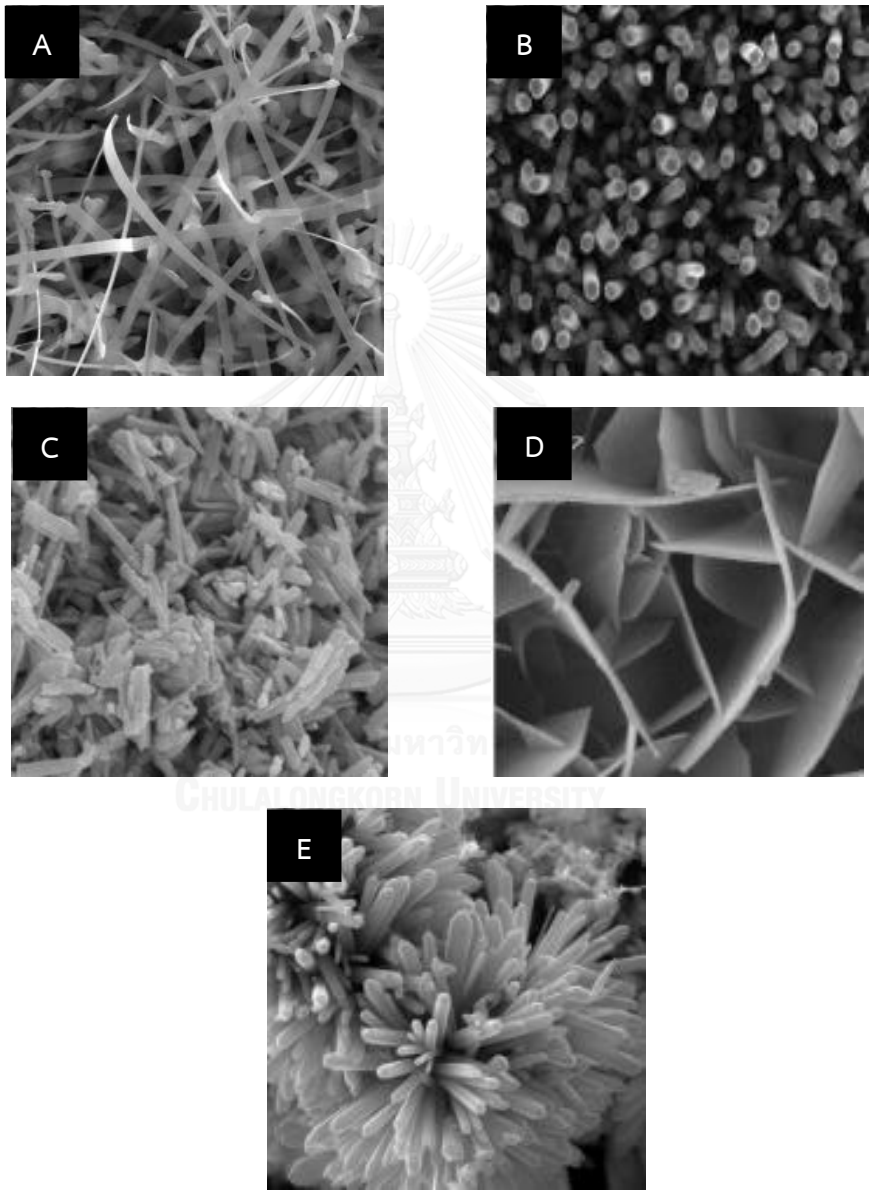

Figure 2.8 Various nanostructure of ZnO including nanobelts (A), nanotubes (B), nanorods (C), nanosheets (D) and nanoflowers (E).

There are many previous researchs using ZnO for electrode surface modification in electrochemical sensor applications. It has been reported that, the ZnO can enhance both electrochemical conductivity and electrocatalytic activity of modified electrode.

Arabali et al. [46] developed a highly sensitive determination of promazine by using ZnO nanoparticle modified ionic liquid carbon paste electrode. The results showed that, the presence of ZnO nanoparticle on electrode surface can increase the electrochemical sensivitiy 4 times higher than the unmodified surface of carbone paste electrode in the determination of promazine. It was found that, the ZnO nanoparticles can enhance the electrochemical sensitivity in the detection of promazine.

Liu et al. [42] developed an electrochemical sensor based on ZnO nanofiber modified glassy carbon electrode for determination of trace Cd^{2+}. From the results, the ZnO nanofiber/ Nafion modified GCE exhibited a large specific surface area leading to rich active sites. Moreover, the current response obtained from ZnO nanofiber/Nafion modified glassy carbon electrode on determination of Cd^{2+} was 3-folds higher than the current response obtaind from Nafion modified glassy carbon electrode indicating that, the presence of ZnO can enhance the electrochemical sensitivity for determination of Cd^{2+}.

Recently, there are previous reports using hybrid structure of ZnO and graphene for working electrode surface modification. The results showed that, the presence of both ZnO and graphene can increase the specific surface area and also enhance the electrochemical sensitivity by their synergistic effect.

Zhang et al. [28] developed an electrochemical sensor based on reduced graphene oxide (RGO)/ZnO composite modified glassy carbon electrode for simultaneous detection of ascorbic acid, dopamine and uric acid. The hybrid structure of ZnO and RGO could largely enhance the electroactive surface area leading to high electrochemical sensitivity for simultaneous determination of ascorbic acid, dopamine and uric acid. Moreover, this prepared electrode displayed a good reproducibility and stability and successfully used as an electrochemical biosensor.

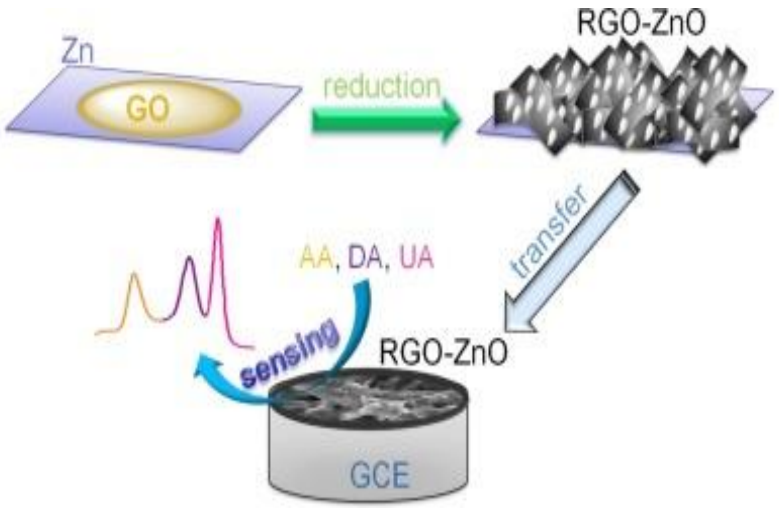

Figure 2.9 Schematic illustration of fabrication process the RGO/ZnO modified glassy carbon electrode as an electrochemical biosensor.

Lu et al. [47] developed an electrochemical sensor based on ZnO nanotubes and graphene composite modified electrode for detection of trace Pb^{2+}. From the results, this electrode showed high specific surface area due to its high porosity leading to high specific surface area. Moreover, the ZnO/G based electrode prepared in this study showed highly sensitive for the detection of Pb^{2+}

Moreover, among many shapes of ZnO nanostructures, the ZnO nanorods can form three dimensional (3D) structure after combining with graphene to obtain extremely large surface area [23]. Thus, in this study we focused on using ZnO/G nanocomposite for electrode surface modification to improve the electrochemical sensitivity in an electrochemical sensor application.

2.5 Toxic heavy metals

Toxic heavy metals, such as cadmium (Cd^{2+}) and lead (Pb^{2+}), are metallic element with high density that produced from several industrial factories such as weaving, pigment and battery. These heavy metals can cause serious problem for environment and human health even at trace level. Moreover, these heavy metals are non-biodegradable and very difficult to be eliminated. Thus, the natural resources can be easily contaminated by these toxic heavy metals. Besides, the accumulation of these heavy metals in human body can cause diseases to several organs such as liver,

kidney, bone and skin. There are many several methods used for heavy metal detection such as inductively coupled plasma-mass spectrometry (ICP-MS), atomic absorption spectroscopy (AAS), inductively coupled plasma optical emission spectroscopy (ICP-OES) and etc. These techniques provide the high sensitivity and selectivity. However, these techniques require specialized operator, high operating cost and long analysis time. Thus, the electrochemical detection has become an alternative device for heavy metal detection due to its simplicity, high sensitivity, rapid analysis and also inexpensive process cost. There are previous works using mercury electrode for heavy metals detection in electrochemical analysis. This technique provides the high sensitivity and high selectivity for simultaneous detection of heavy metals. However, this mercury electrode are also dangerous because mercury is one of the most toxicity heavy metals leading to high risk operation [48]. Later, bismuth is used for electrode modification instead of using mercury electrode due to its non-toxicity, environmental friendly and also high analytical performance of heavy metal detection [49]. There are two ways in previous reports using bismuth in the detection of target heavy metal including *in-situ* and *ex-situ* bismuth modified electrode [50]. In the first way, *in situ* bismuth modified electrode, the bismuth is directly mixed with target heavy metals solution to form amalgamated film on electrode surface during preconcentration step in anodic stripping voltammetry measurement.

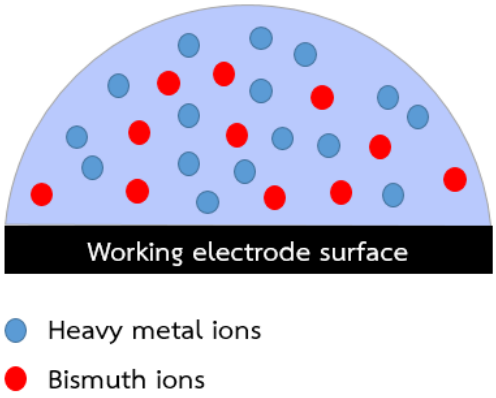

Figure 2.10 The *in situ* bismuth modified electrode.

In the second way, *ex situ* bismuth modified electrode, bismuth is deposited on electrode surface as thin film by electro-deposition method. After that, bismuth modified electrode is used for the detection of target heavy metals.

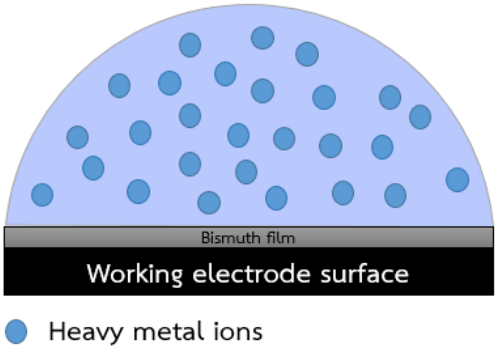

Figure 2.11 The *ex situ* bismuth modified electrode.

CHAPTER III

EXPERIMENTAL

In this chapter, the detail of the experiments including, reagents, raw materials, instruments, equipment and preparation process were provided.

3.1 Reagents and materials

- Graphene (G) nanopowder (SkySpring Nanomaterials Inc, Houston, Tx, USA)
- Zinc acetate ($Zn(CH_3COO)_2$) (Ajax Finechem Pty Ltd., Auckland, New Zealand)
- Zinc chloride ($ZnCl_2$) (Carlo Erba reagent, Milano, Italy)
- Acetic acid (CH_3COOH) (Carlo Erba reagent, Milano, Italy)
- Sodium acetate (CH_3COONa) (Carlo Erba reagent, Milano, Italy)
- Cadmium (Cd^{2+}) 1000 mgL^{-1} standard solution (VWR International Ltd., Poole, England)
- Lead (Pb^{2+}) 1000 mgL^{-1} standard solution (VWR International Ltd., Poole, England)
- Bismuth (Bi^{3+}) 1000 mgL^{-1} standard solution (VWR International Ltd., Poole, England)
- Carbon graphene ink (Gwent group, Torfaen, United Kingdom)
- Silver/silver chloride (Ag/AgCl) ink (Gwent group, Torfaen, United Kingdom)
- Filter paper Whatman grade 5 (GE healthcare Bio-Sciences, Pittsburgh, PA)
- Potassium chloride (KCl) (PFCL Ltd., New Deli, India)

- Potassium ferricyanide ($K_3[Fe(CN)_6]$) (Sigma-Aldrich, St. Louis, Mo, USA)
- Potassium ferrocyanide ($K_4[Fe(CN)_6]$) (Sigma-Aldrich, St. Louis, Mo, USA)
- Sodium dodecyl sulfate (SDS) (Sigma-Aldrich, St. Louis, Mo, USA)
- Hydrochloric acid (HCl) (Carlo Erba reagent, Milano, Italy)

3.2 Instruments and equipment

- Scanning electron microscopy (SEM) with Energy dispersive X-ray spectroscopy (EDX) JSM-6400 (Japan Electron Optics Laboratory Co., Ltd., Japan)
- Transmission electron microscopy (TEM), JEM-2100 (Japan Electron Optics Laboratory Co., Ltd., Japan)
- X-ray diffractrometry (XRD) (STREC, Chulalongkorn University)
- 910 PSTAT mini (Metrohm Siam Company Ltd.)
- Inductively coupled plasma optical emission spectroscopy (ICP-OES)

3.3 Preparation of solution

All of aqueous solutions were prepared by using Milli-Q water (12.8 MΩ cm).

3.3.1 Preparation of $ZnCl_2$ solution (0.001 M)

0.136 g of $ZnCl_2$ was dissolved in 1000 mL of water with stirring for 30 min.

3.3.2 Preparation of ZnO solution (0.5 mg/ml)

50 mg of ZnO nanorods were dispersed in 100 mL of 0.001M $ZnCl_2$ solution with stirring and ultrasonincation for 2 hrs.

3.3.3 Preparation of G solution (0.5 mg/ml)

50 mg of SDS and 50 mg of G nanopowders were added in to 100 mL of water and stirring for 30 min. After that, the G solution was ultrasonicated for 24 hrs.

3.3.4 Preparation of 2 M acetic acid solution

2.29 mL of 17.5 M acetic acid solution was added to 17.71 mL of water to prepare 20 mL of 2 M acetic acid solution.

3.3.5 Preparation of 2 M sodium acetate solution

3.28 g of sodium acetate was dissolved in 20 mL of water to prepare 20 mL of 2 M sodium acetate solution.

3.3.6 Preparation of 0.1 M acetate buffer solution pH 4.5

2.95 mL of 2 M acetic acid solution and 2.05 mL of 2 M sodium acetate solution were dissolved in 95 mL of water to obtain 0.1 M acetate buffer solution pH 4.5. This solution was used as a supporting electrolyte for simultaneous determination of Cd^{2+} and Pb^{2+}.

3.3.7 Preparation of 0.5 M potassium chloride solution

9.32 g of KCl was dissolved in 250 mL of water to obtain 0.5 M of KCl solution. The 0.5 M of KCl was used as a supporting electrolyte of ferri/ferro cyanide for CV measurement. Moreover, this solution was diluted to 0.1 M KCl and used for study the effect of supporting electrolyte in simultaneous detection of Cd^{2+} and Pb^{2+}.

3.3.8 Preparation of 5 mM of ferri/ferro cyanide redox couple

0.165 g of $K_3[Fe(CN)_6]$ and 0.211 g of $K_4[Fe(CN)_6]$ were dissolved in 100 mL of 0.5 M KCl solution. Then, stock solution of 5 mM of ferri/ferro cyanide was obtained.

3.3.9 Preparation of 0.1 M phosphate buffer solution (PBS) pH 7.0

2.083 g of Na_2HPO_4 and 1.405 g of KH_2PO_4 were dissolved in 250 mL of water and adjusted to pH 7.0 by using 0.1 M HCl. Then, the 0.1 M PBS pH 7.0 was obtained.

3.3.10 Preparation of stock standard solution of cadmium and lead

1000 mg·L^{-1} of stock standard solution of Cd^{2+} and Pb^{2+} were diluted to 1 mg·L^{-1} by using a supporting electrolyte (e.g. Acetate buffer solution, HCl). Then, 1 mg·L^{-1} of Cd^{2+} and Pb^{2+} were mixed to prepare mixed solution of Cd^{2+} and Pb^{2+}. Finally, 0.5 mg·L^{-1} of standard stock solution of Cd^{2+} and Pb^{2+} was obtained.

3.3.11 Preparation of stock standard solution of bismuth

1000 mg·L^{-1} of stock standard solution of Bi^{3+} was diluted to 1 mg·L^{-1} by 0.1 M acetate buffer solution pH 4.5. This solution was used for in-situ plating of Bi^{3+}.

3.4 Synthesis of ZnO nanorods

ZnO nanorods were synthesized following by thermal decomposition method [51]. Initially, 5 g of zinc acetate dihydrate was grinded for 30 min to get fine white powder. Then, the white powder was calcined in furnace by heating rate of 5 ºC min^{-1} till 350 ºC and held for 3 hrs. After that, it was cooled to room temperature by air. Finally, the obtained powder was washed by absolute ethanol at least 3 times and dried at 80 ºC for 8 hrs. The gray powder of ZnO nanorod was obtained.

3.5 Synthesis of ZnO/G nanocomposite

ZnO solution (0.5 mg/mL) was added in to G solution (0.5 mg/mL) along with stirring for 30 min. Then, stop stirring and waiting for the sediment settled down at the bottom of beaker. After that, the sediment was washed by absolute ethanol at least 3 times and dried at 80 ºC for 8 hrs. The synthesized ZnO/G nanocomposites were obtained. Moreover, the ratio of ZnO and G was controlled by the volume of ZnO solution and G solution. For example, to prepare ZnO/G ratio at 70:30, 70 mL of ZnO solution was added in to 30 mL of G solution.

3.6 Fabrication of screen-printed carbon electrode

The screen-printed carbon electrodes (SPCE) were fabricated by using an in-house screen-printing technique as shown in Figure 3.1. The electrode formation was designed by Adobe Illustrator. Firstly, Ag/AgCl was screened on PVC substrate as reference electrode and conductive pad, then dried at 50°C. After that, carbon ink was screened over conductive pad as counter electrode and working electrode. Finally, they were dried at 50°C for 1 hrs. [5].

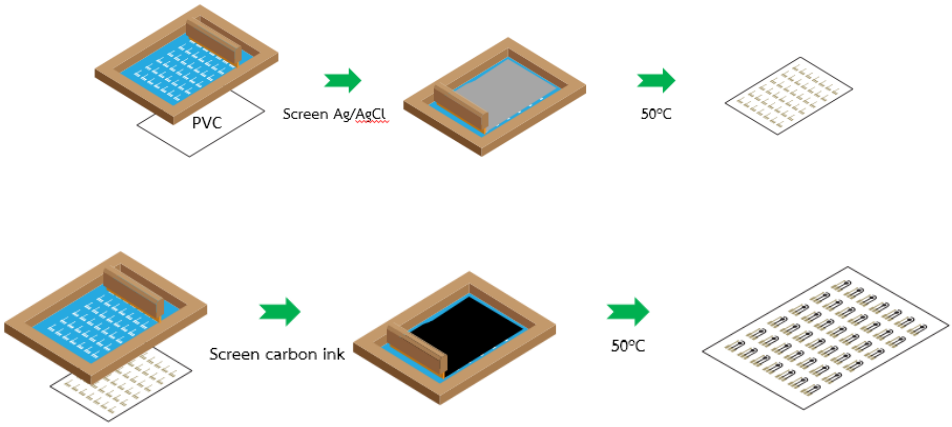

Figure 3.1 Fabrication procedure of SPCE using in-house screen printing technique.

3.7 Fabrication of ZnO/G modified electrode

ZnO/G nanocomposites were dispersed in 1 ml of absolute ethanol and ultrasonicated for at least 2 hrs. to obtain the dispersed ZnO/G solution. To prepare the ZnO/G modified electrode, 1 µL of dispersed ZnO/G solution was dropped-coating on working electrode surface and dried at room temperature. The ZnO/G modified electrode was obtained. Likewise, G modified electrode was prepared by similar method without mixing with ZnO.

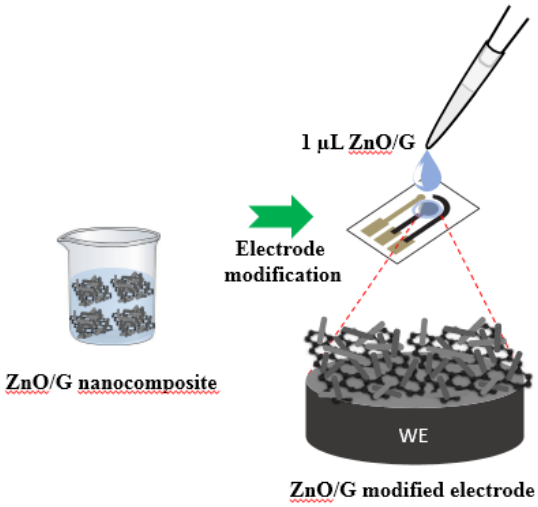

Figure 3.2 The procedure of electrode surface modification by using ZnO/G.

3.8 Optimization of modified electrode and electrochemical parameters

All of parameters affecting on electrochemical sensitivity of simultaneous detection of Cd^{2+} and Pb^{2+} was studied by using ASV measurement.

3.8.1 Effect of ZnO/G ratio

The ratio of ZnO and G was controlled by volume of ZnO solution and G solution during preparation step. The influence of different ratios at 90:10, 80:20, 70:30, 60:40 and 50:50 on electrochemical sensitivity were studied and optimized.

3.8.2 Effect of ZnO/G concentration

The influence of different concentration of ZnO/G at 1, 2, 3 and 4 mg/mL on electrochemical sensitivity were studied. For example, to prepare ZnO/G at 1 mg/mL, 1 mg of ZnO/G nanocomposite was dispersed in 1 mL of ethanol and ultrasonicated for 2 hrs.

3.8.3 Effect of supporting electrolyte

Various types of supporting electrolyte including hydrochloric acid, acetate buffer, potassium chloride and phosphate buffer saline affecting on electrochemical behavior both peak shape and sensitivity were studied and investigated. These electrolytes were used to dilute the target analyte on ASV measurement.

3.8.4 Effect of bismuth concentration

In this study, the Bi^{3+} was added into mixed solution of Cd^{2+} and Pb^{2+} to enhance the electrochemical sensitivity of Cd^{2+} and Pb^{2+}. The effect of Bi^{3+} concentrations were studied and also investigated at 250, 500, 750, 1000 and 1250 $\mu g \cdot L^{-1}$.

3.8.5 Effect of electrochemical parameters

The electrochemical parameters affecting on electrochemical sensitivity for simultaneous detection of 50 $\mu g \cdot L^{-1}$ of Cd^{2+} and Pb^{2+} with 1000 $\mu g \cdot L^{-1}$ of Bi^{3+} were investigated by using ASV. The deposition potential in the range from -1.5 to -1.0 V, the deposition time in the range 60 to 300 s, the step potential in the range from 5 to 20 mV, frequency in the range 10 to 90 Hz and the potential amplitude in the range 20 to 80 mV were studied and optimized.

3.9 Characterization of materials and modified electrode

3.9.1 Surface morphology characterization

The morphology of ZnO nanorods, ZnO/G nanocomposite, unmodified SPCE and ZnO/G modified SPCE were characterized by SEM and TEM. Moreover, the average size of ZnO nanorods were calculated by using SemAfore 5.21 software.

3.9.2 Electrochemical characterization

910 PSTAT mini was used to study all of electrochemical measurements using CV and ASV that controlled by 910 PSTAT software. Initially, CV was used to preliminary study the electrochemical response from unmodified SPCE and ZnO/G modified SPCE by using standard solution of 1.0 mM $[Fe(CN)_6]^{3-/4-}$ in 0.5 M KCl (supporting electrolyte) over a potential range of -0.5 to +1 V and a scan rate of 100 $mV \cdot s^{-1}$. Moreover, the simultaneous detection of 50 $\mu g \cdot L^{-1}$ of Cd^{2+} and Pb^{2+} was studied by using ASV with optimum conditions.

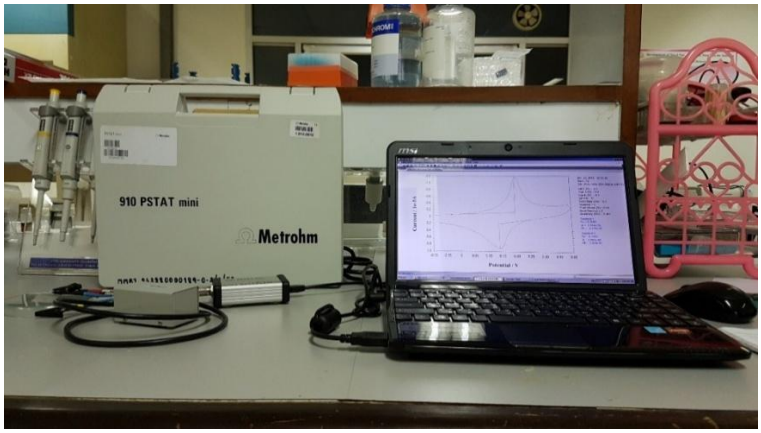

Figure 3.3 The equipment of electrochemical system used in this study.

3.10 The analytical performance of ZnO/G modified SPCE

3.10.1 Calibration plot

Firstly, 500 $\mu g \cdot L^{-1}$ of stock standard solution of mixed solution (Cd^{2+} and Pb^{2+}) was diluted to different concentrations (10-200 $\mu g \cdot L^{-1}$) and measured on ZnO/G modified SPCE under optimum conditions. Then, the graph is plotted between anodic current response and concentration of target heavy metal. Finally, the linear range of this system was obtained.

3.10.2 Limit of detection

The limit of detection (LOD) is calculated by using the formula of LOD = $3S.D._b/M$, where $S.D._b$ is the standard deviation from the blank measurement (at least seven times) and M is a slope of calibration curve.

3.10.3 Repeatability

To study the repeatability, the same ZnO/G modified SPCE was used to detect the target analyte at least 10 times and reported as the percentage of relative standard deviation (%RSD) which is calculated by the formula %RSD = (standard deviation x $mean^{-1}$) x 100

3.10.4 Interference study

Normally, there are many ions existing in real water sample such as Na^+, K^+, Ca^{2+}, Mg^{2+}, Ba^{2+},Cu^{2+}, Co^{2+}, Ni^{2+}, Zn^{2+}, Mn^{2+}, Fe^{2+}, Fe^{3+}, Cl^-, SO_4^{2-}, NO_3^- which might interfere the current response of target heavy metal in ASV. Therefore, the effect of other ions on the simultaneous detection of Cd^{2+} and Pb^{2+} were investigated and reported as tolerance ratio (±5% signal response change was acceptable).

3.11 Real sample analysis

3.11.1 Preparation of wastewater samples

The wastewater samples were acquired from different textile factories in Thailand. To purify the wastewater, the wastewater was filtered by filter paper (grade 5) to remove ashes and residues. Then, the filtered wastewater was prepared in acetate buffer solution (pH 4.5). After that, known amounts of Cd^{2+} and Pb^{2+} (10, 50 and 100 $\mu g \cdot L^{-1}$) were spiked into filtered wastewater samples and evaluated by using standard addition method [3]. To validate with standard technique, the results obtained from proposed method were compared with the results obtained from ICP-OES method.

3.11.2 Recovery

The percentage of recovery was used to verify the applicability of the purposed method in real sample analysis. The % recovery can be calculated by:

$$\% \text{ recovery} = \frac{\text{concentration amount of spiked sample-concentration amount of un-spiked sample}}{\text{known amount of spike value}} \times 100$$

CHAPTER IV
RESULTS AND DISCUSSION

In this chapter, the results including the morphology characterization of synthesized ZnO nanorods and ZnO/G nanocomposites, the optimization of SPCE modification procedures, the optimization of electrochemical parameters, the analytical performances of ZnO/G modified SPCE and application of ZnO/G modified SPCE for simultaneous determination of Cd^{2+} and Pb^{2+} in industrial wastewater samples, were discussed.

4.1 Characterizations of synthesized ZnO nanorods

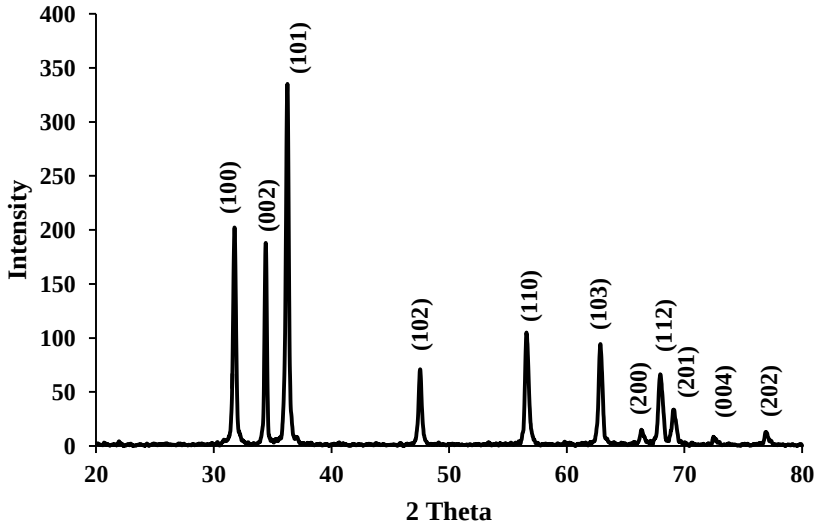

Figure 4.1 XRD pattern of syntheized ZnO.

In this study, ZnO were synthesized by thermal decomposition method using zinc acetate as a precursor [23]. The synthesized ZnO nanorods were characterized by XRD as shown in Figure 4.1. The results obtained from XRD confirming that the as-prepared powder was ZnO. An XRD diffraction pattern displays sharp reflection peaks and appeared at 2 theta = 31.7°, 34.4°, 36.2°, 47.6°, 56.7°, 62.9°, 66.4°, 68.1°, 69.2°, 72.7° and 77.2° corresponded to the (100), (002), (101), (102), (110), (103), (200), (112), (201), (004) and (202) planes of ZnO wurtzite structure as described in the previous report [52].

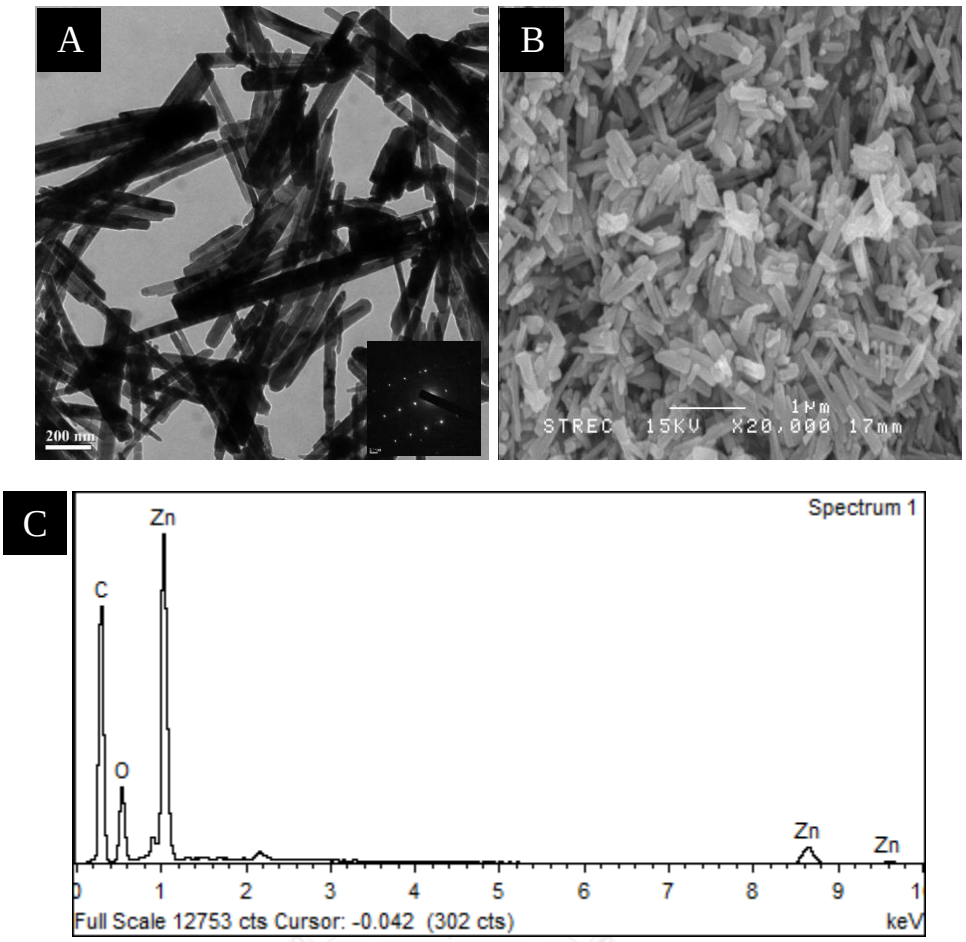

Figure 4.2 TEM (A), SEM (B) and SEM-EDX of ZnO nanorods (C).

Moreover, TEM and SEM were used to study the morphology of the synthesized ZnO nanorods as shown in Figure 4.2A and 4.2B, respectively. The results showed the nanorod structure of the synthesized ZnO with an average diameter size of 93±21 nm uniformly dispersed on the surface. Besides, the results obtained from SEM-EDX clearly showed the characteristic peaks of zinc (Zn) and oxygen (O), as seen in Figure 4.2C, which verify the ZnO structure. After that, ZnO nanorods prepared in this study were used to synthesize ZnO/G nanocomposites in the subsequent experiments.

4.2 Characterization of ZnO/G nanocomposites

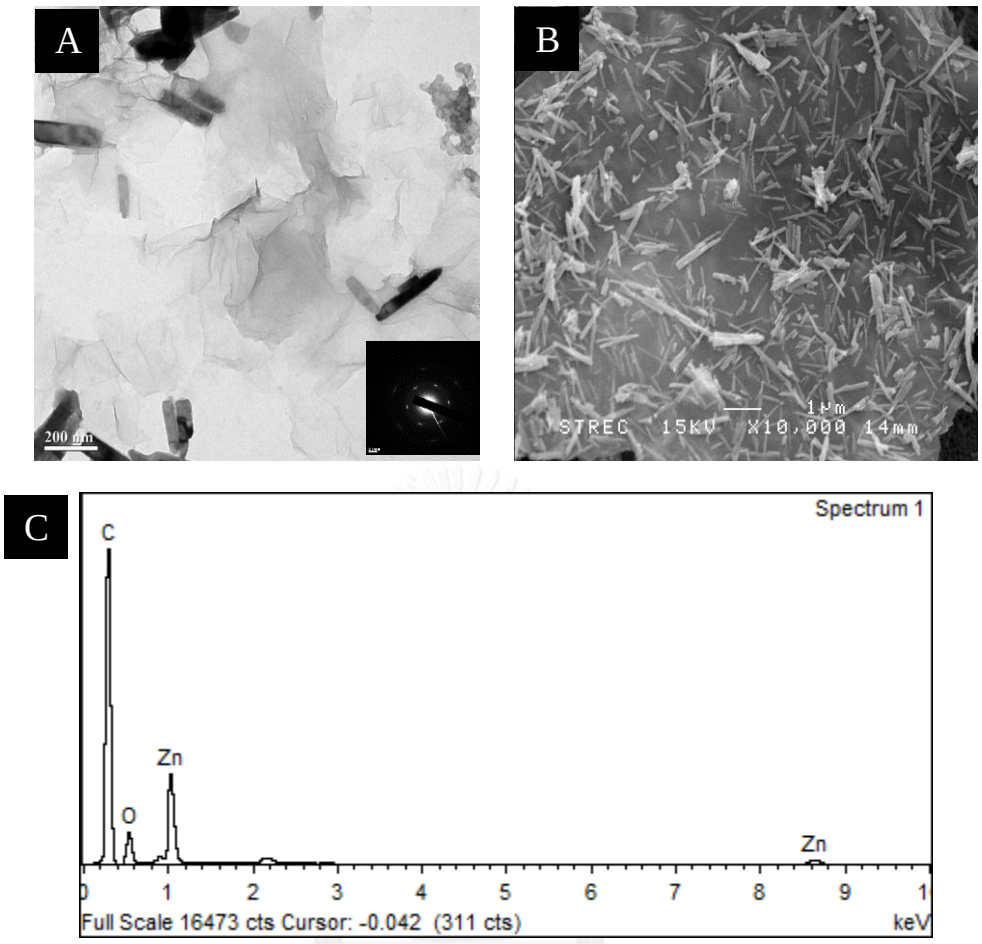

Figure 4.3 TEM (A), SEM (B) and SEM-EDX (C) of synthesized ZnO/G nanocomposites.

The synthesis of ZnO/G nanocomposites were accomplished by mixing ZnO solution with G solution through the colloidal coagulation effect [51]. The morphologies of synthesized ZnO/G nanocomposites were characterized by TEM and SEM as shown in Figure 4.3A and 4.3B, respectively. As seen in Figure 4.3A, the black and the gray rods were ZnO that anchored on G sheets and inserted between the G layers. From SEM image as seen in Figure 4.3B, the obtained results showed that ZnO nanorods uniformly dispersed on both sides of G nanosheets and thoroughly intercalated between G layers. Likewise, ZnO nanorods can act as the pillar to prevent self-agglomeration of G. Moreover, the presence of ZnO nanorods on the G sheets can construct the three dimensional of ZnO/G leading to increase the surface roughness and surface area compared with two dimensional structure of pure G sheet. In addition,

the result obtained from SEM-EDX as seen in Figure 4.3C, showed the characteristic peaks of Zn, O and C. These peaks can confirm the presence of ZnO/G nanocomposite on the surface. Subsequently, ZnO/G nanocomposites were further used for electrode surface modification to increase the analytical performance of this developed sensor.

4.3 Electrochemical sensor based on ZnO/G nanocomposite modified SPCE

Firstly, CV was used to preliminary study the ZnO/G nanocomposite modified SPCE by using a standard solution of 0.1 mM $[Fe(CN)_6]^{3-/4-}$ in 0.1 M KCl as a redox couple. The results obtained from CV showed the electrochemical responses of unmodified SPCE comparing with G modified SPCE and ZnO/G modified SPCE as shown in Figure 4.4. The results showed that, the anodic peak current response of G modified SPCE was higher than unmodified SPCE leading to increased electrochemical sensitivity. However, ZnO/G nanocompositemodified SPCE showed the highest peak current response indicating that, the electrochemical property of G can be further enhanced by ZnO. Thus, this novel electrode was applied for the detection of target analytes in the next step.

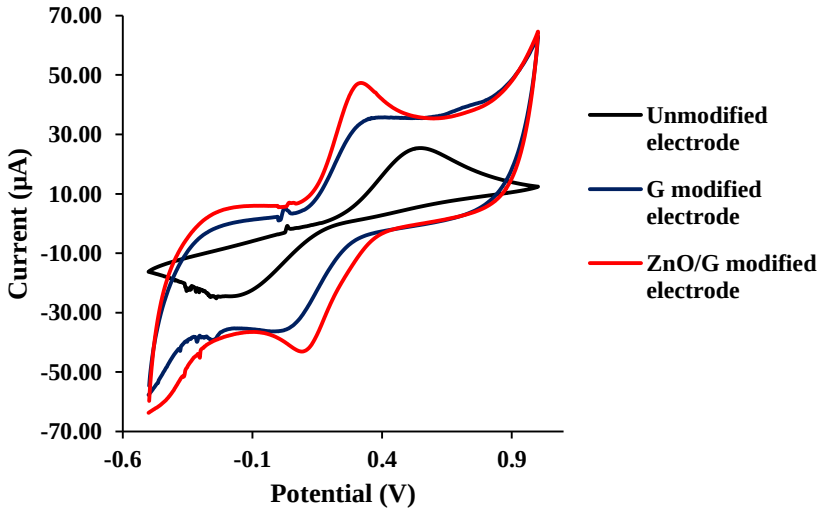

Figure 4.4 Cyclic voltammograms of 1.0 mM $[Fe(CN)_6]^{3-/4-}$ in 0.5 M KCl using unmodified SPCE, G modified SPCE and ZnO/G modified SPCE.

4.3.1 Electrochemical determination of Cd^{2+} and Pb^{2+}

Herein, we focused on the simultaneous determination of Cd^{2+} and Pb^{2+} by using ZnO/G modified SPCE. ASV, one of the electrochemical techniques, which has been widely used for heavy metals determination since the heavy metals can be accumulated on the working electrode surface during pre-concentration step causing the increase in electrochemical sensitivity of the sensor. Thus, this technique was chosen for the simultaneous determination of Cd^{2+} and Pb^{2+} in this study.

To obtain the highest sensitivity for simultaneous determination of Cd^{2+} and Pb^{2+}, all parameters, including ZnO/G ratio, ZnO/G concentration, Bi^{3+} concentration, and other electrochemical parameters, affecting on electrochemical sensitivity of ZnO/G modified SPCE were investigated and optimized.

4.3.2 Optimization of ZnO/G nanocomposite modified SPCE

4.3.2.1 Effect of ZnO/G ratio

From the previous step, ZnO/G nanocomposites were prepared by mixing of ZnO solution (0.5 mg/mL) and G solution (0.5 mg/mL) to obtain the ZnO/G ratio at 50:50. However, the ratio of ZnO/G can be adjusted by the change of volume of ZnO and G solution. To study the effect of ZnO/G ratio on the electrochemical sensitivity of this sensor, ZnO/G nanocomposites were prepared at different ratio including 90:10, 80:20, 70:30, 60:40 and 50:50. Then, these prepared nanocomposites were used to modify the working electrode surface by simply drop-coating. The electrode surface of unmodified SPCE and various ratio of ZnO/G modified SPCE were characterized by SEM as shown in Figure 4.5A and 4.5B-F, respectively. Afterwards, the suitable ratio between ZnO and G providing the highest electrochemical sensitivity was investigated and optimized using ASV.

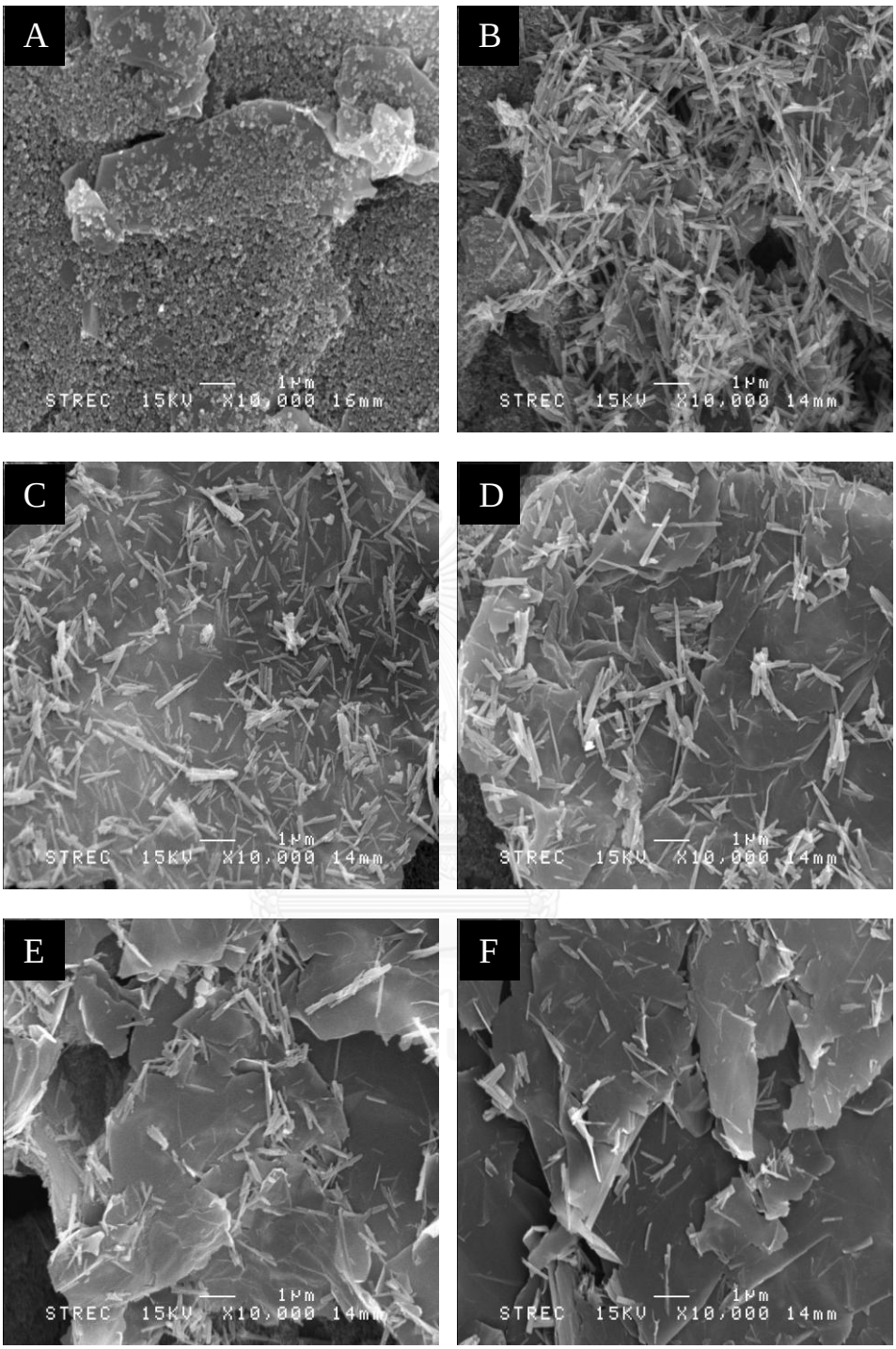

Figure 4.5 SEM images of unmodified SPCE (A) and ZnO/G modified SPCE at different ratio including 90:10 (B), 80:20 (C), 70:30 (D), 60:40 (E) and 50:50 (F).

Afterwards, ASV was used for the simultaneous determination of 50 μg·L^{-1} of $Cd^{2+}$and Pb^{2+} in the presence of 500 μg·L^{-1} of Bi^{3+}. The results obtained from ASV were shown in Figure 4.6 (left). The anodic peak potential of Cd^{2+} and Pb^{2+} were measured at -1.1 and -0.8 V, respectively. Moreover, the anodic peak current response obtained from ASV was plotted in the bar graph as seen in Figure 4.6 (right). The results showed that, the peak current response increases with increasing of G composition from 10 to 20 %. It was found that, G can enhance the electrochemical sensitivity of this system due to its high conductivity. However, the current response decreases when G proportion is higher than 20 %, which is probably because the high percentage of G can increase the chance of self-agglomeration indicated by the high background current signal. Thus, the suitable ratio of ZnO/G modified SPCE was 80:20 and this ratio will be used in all further experiments.

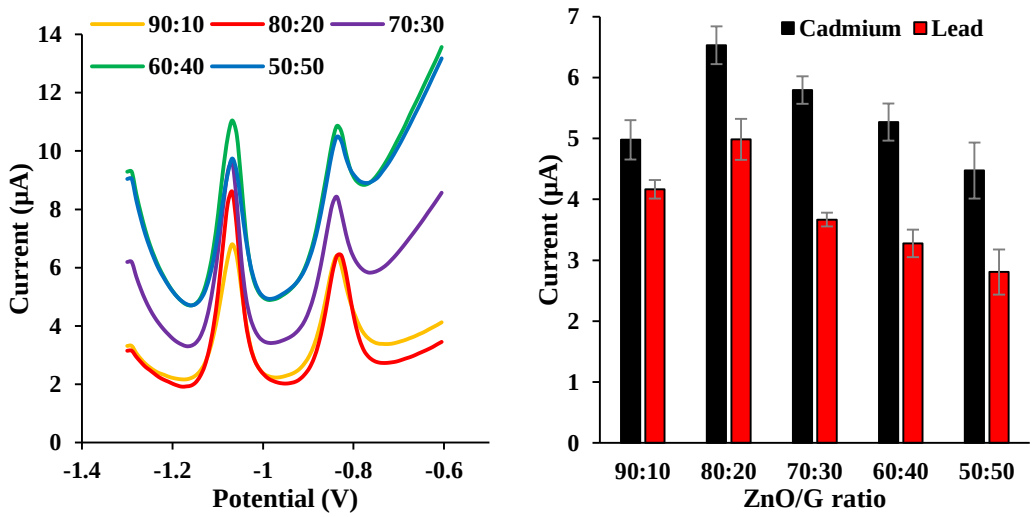

Figure 4.6 Effect of ZnO/G ratio on stripping peak of 50 μg·L^{-1} Cd^{2+} and Pb^{2+} with Bi^{3+} 500 μg·L^{-1} in 0.1 M acetate buffer solution (pH 4.5). The error bars correspond to the standard deviation obtained from 3 measurement (n=3).

4.3.1.2 Effect of ZnO/G concentration

An effect of ZnO/G concentration on the working electrode surface was studied by ASV for the simultaneous determination of 50 $\mu g \cdot L^{-1}$ of Cd^{2+} and Pb^{2+}. The concentration of Bi^{3+} was fixed at 500 $\mu g \cdot L^{-1}$. In this study, 1 µL of dispersed ZnO/G solution was dropped coating on working electrode surface. The concentration of dispersed ZnO/G solution was varied in a range of 1, 2, 3 and 4 mg/mL as shown in Figure 4.7 (left) and the bar graphs of the anodic peak current response obtained from ASV were shown in Figure 4.7 (right). From the results, the peak current responses increase with increasing the concentration of ZnO/G from 1 to 2 mg/mL, indicating that adding ZnO/G on the working electrode surface can enhance the electrochemical sensitivity due to its high surface area and high conductivity. However, the peak currents decrease when the concentration of ZnO/G is more than 2 mg/mL. Because the high content of ZnO/G on electrode surface possibly increase in the thickness of electrode surface, leading to low electrochemical sensitivity. Thus, an optimum concentration of ZnO/ G was 2 mg/mL and this concentration will be used in all next experiments.

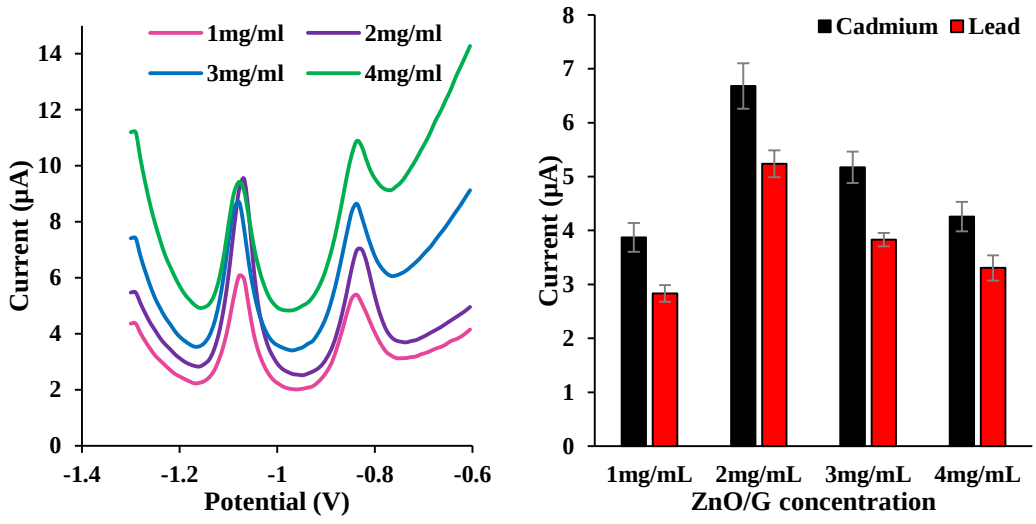

Figure 4.7 Effect of ZnO/G concentration on stripping peak of 50 $\mu g \cdot L^{-1}$ of Cd^{2+} and Pb^{2+} with Bi^{3+} 500 $\mu g \cdot L^{-1}$ of in 0.1 M acetate buffer solution (pH 4.5). The error bars correspond to the standard deviation obtained from 3 measurement (n=3).

4.3.3 Optimization of affecting parameters on electrochemical sensitivity

To obtain the highest electrochemical sensitivity of ZnO/G modified electrode for the simultaneous determination of Cd^{2+} and Pb^{2+}, other electrochemical factors, including the type of supporting electrolyte, deposition potential, deposition time, frequency, potential amplitude, step potential and concentration of Bi^{3+} were also investigated.

4.3.3.1 Effect of supporting electrolyte

An effect of supporting electrolyte in the simultaneous determination of 50 $\mu g \cdot L^{-1}$ of Cd^{2+} and Pb^{2+} on ZnO/G modified SPCE was investigated by using various types of supporting electrolyte including 0.1 M acetate buffer solution pH 4.5, 0.1 M HCl pH 1.0 and 0.1 M KCl pH 7.0 as shown in Figure 4.8 (left) while the concentration of Bi^{3+} was fixed at 1000 $\mu g \cdot L^{-1}$.The current response obtained from AVS were plotted as the bar graph as shown in Figure 4.8 (right). From the results, the well-defined peak obtained when 0.1 M Acetate buffer solution was used as a supporting electrolyte. Among the supporting electrolytes, acetate buffer showed highest peak current response. Thus, 0.1 M acetate buffer solution (pH 4.5) was selected as a supporting electrolyte for all ASV experiments.

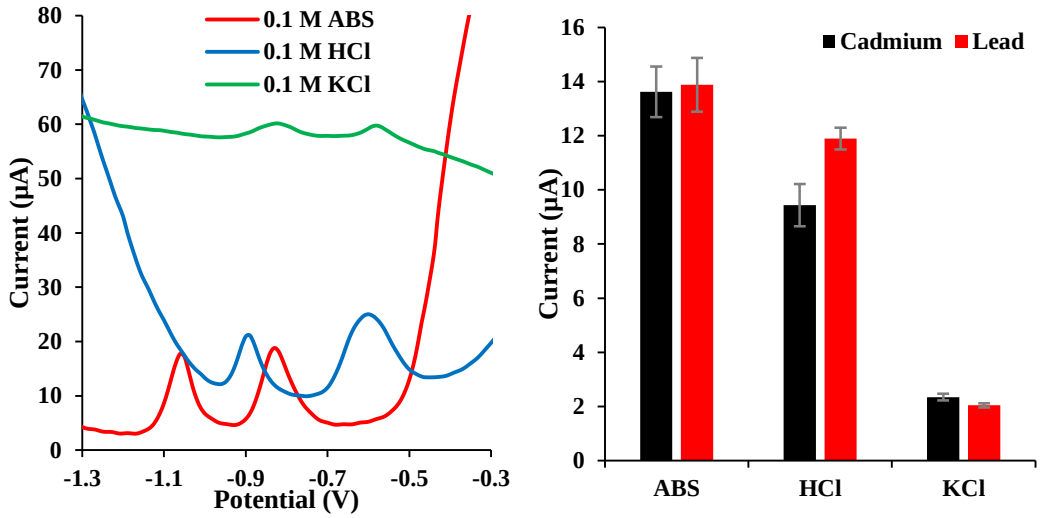

Figure 4.8 Effect of various supporting electrolytes on stripping peak of 50 µg·L^{-1} of Cd^{2+} and Pb^{2+} with Bi^{3+} 1000 µg·L^{-1} in 0.1 M acetate buffer solution (note as ABS) pH 4.5, 0.1 M HCl pH 1.0 and 0.1 M KCl pH 7.0. The error bars correspond to the standard deviation obtained from 3 measurement (n=3).

4.3.3.2 Effect of deposition potential

An effect of deposition potential on anodic stripping peak current was investigated by ASV for the simultaneous determination of 50 µg·L^{-1} Cd^{2+} and Pb^{2+} while the concentration of Bi^{3+} was fixed at 500 µg·L^{-1}. The deposition potential was studied in a range from -1.0 to -1.6 V as shown in Figure 4.9 (left). The current response obtained from ASV was plotted as a line graph as shown in Figure 4.9 (right). From the results, the current response of Cd^{2+} and Pb^{2+} immediately increases when the applied potential change from -1.0 to -1.2 V and gradually decreases when the applied potential more negative than -1.2 V due to the hydrogen formation. The electrode surface was partially covered by hydrogen bubbles that can potentially interfere the system. Thus, -1.2 V of deposition potential was chosen as an optimal potential for all subsequent experiments.

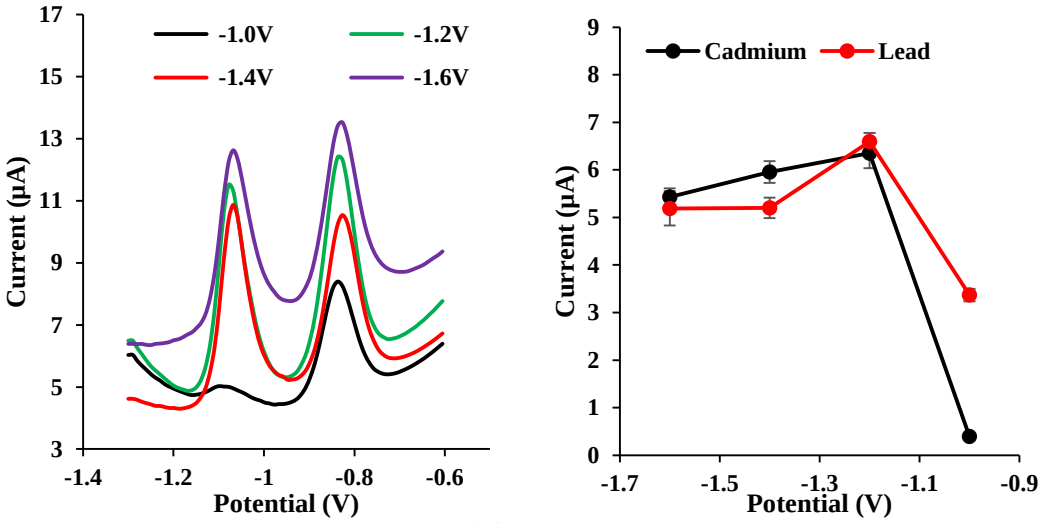

Figure 4.9 Effect of deposition potential on stripping peak of 50 µg·L^{-1} of Cd^{2+} and Pb^{2+} with Bi^{3+} 500 µg·L^{-1} in 0.1 M acetate buffer solution (pH 4.5). The error bars correspond to the standard deviation obtained from 3 measurement (n=3).

4.3.3.3 Effect of deposition time

The influence of deposition time was investigated by ASV for the simultaneous determination of 50 µg·L^{-1} Cd^{2+} and Pb^{2+} while the concentration of Bi^{3+} was fixed at 500 µg·L^{-1}. The deposition time was studied in a range from 60 to 300 s. The obtained results from ASV was shown in Figure 4.10 (left). And the current response obtained from ASV was plotted in the line graph as seen in Figure 4.10 (right). The results showed the peak current response obtained from both Cd^{2+} and Pb^{2+} abruptly increase from 60 to 180 s and then gradually increase from 180 s to 300 s because the long accumulation time can be collected almost all of target heavy metals in the system leading to high current response. However, to provide the high electrochemical sensitivity compromising with a relatively short analysis time, the deposition time at 180 s was acceptable and selected as an optimal deposition time for all further experiments.

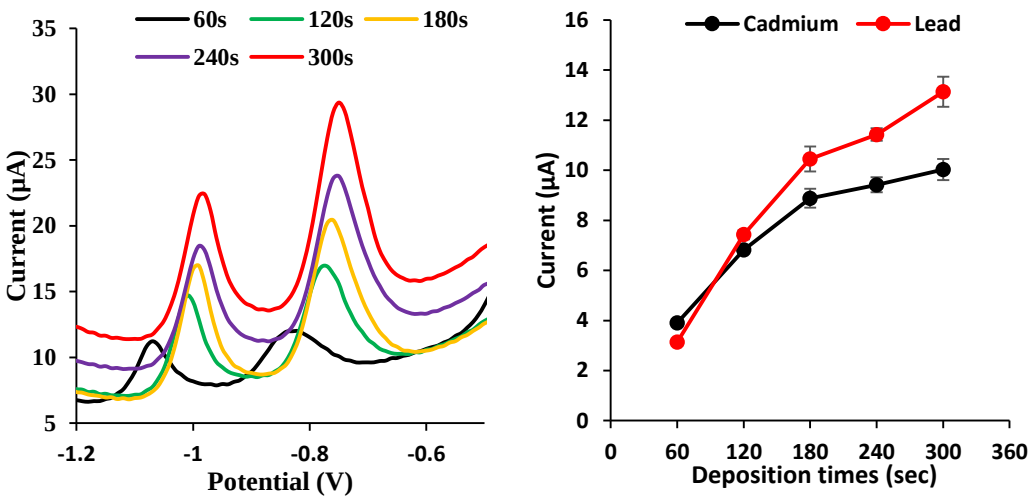

Figure 4.10 Effect of deposition time on stripping peak of 50 µg·L^{-1} of Cd^{2+} and Pb^{2+} with Bi^{3+} 500 µg·L^{-1} in 0.1 M acetate buffer solution (pH 4.5). The error bars correspond to the standard deviation obtained from 3 measurement (n=3).

4.3.3.4 Effect of Frequency

The influence of frequency on the simultaneous determination of 50 µg·L^{-1} Cd^{2+} and Pb^{2+} was investigated and optimized in a range from 10 to 90 Hz by using ASV while the concentration of Bi^{3+} was fixed at 500 µg·L^{-1}. The ASV results was shown in Figure 4.11 (left). The current response obtained from ASV measurement was plotted in the line graph as seen in Figure 4.11 (right). The results showed the electrochemical current responses increase with the increase of frequency for both Cd^{2+} and Pb^{2+}. However, the frequency of this equipment was limited. Therefore, 90 Hz was used as an optimum frequency for all further experiments.

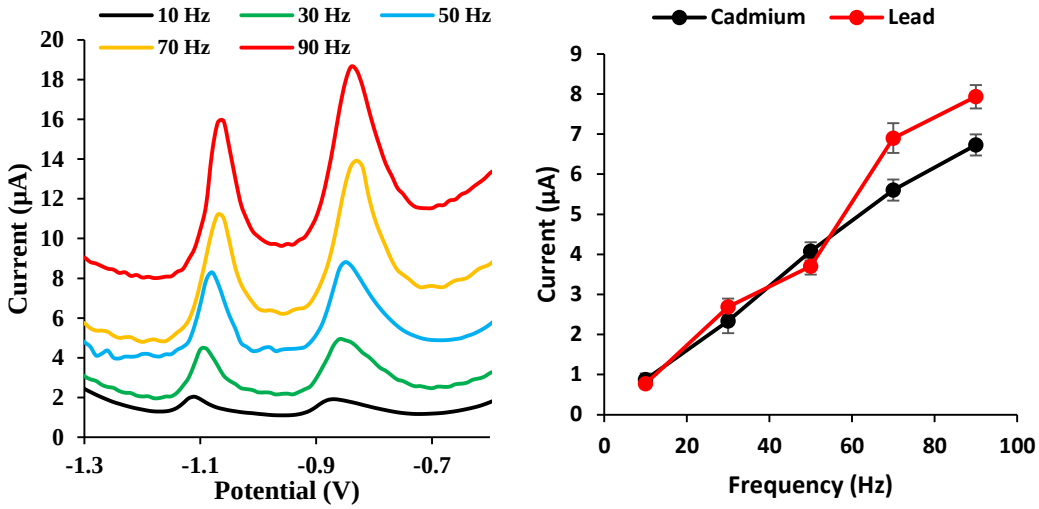

Figure 4.11 Effect of frequency on stripping peak of 50 µg·L^{-1} Cd^{2+} and Pb^{2+} with Bi^{3+} 500 µg·L^{-1} in 0.1 M acetate buffer solution (pH 4.5). The error bars correspond to the standard deviation obtained from 3 measurement (n=3).

4.3.3.5 Effect of Bi^{3+} concentration

Another important parameter was the concentration of Bi^{3+}. The presence of Bi^{3+} in system can improve the detection performance of Cd^{2+} and Pb^{2+} because the Bi^{3+} can form the fused alloy with heavy metal such as Cd^{2+} and Pb^{2+} on working electrode surface during pre-concentration step in ASV [3, 53]. In this study, the concentration of Bi^{3+} was varied from 250 to 1250 µg·L^{-1}. The results obtained from ASV were shown in Figure 4.12 (left). The current response from ASV was plotted in the line graph as shown in Figure 4.12 (right). From the results, the anodic current response obtained from both Cd^{2+} and Pb^{2+} substantially increase from 250 to 1000 µg·L^{-1}. However, at the concentration of Bi^{3+} higher than 1000 µg·L^{-1}, the current response of both Cd^{2+} and Pb^{2+} gradually decrease possibly due to the excess amount of Bi^{3+}. Therefore, a concentration of Bi3+ at 1000 µg·L^{-1} was chosen for all subsequent experiments.

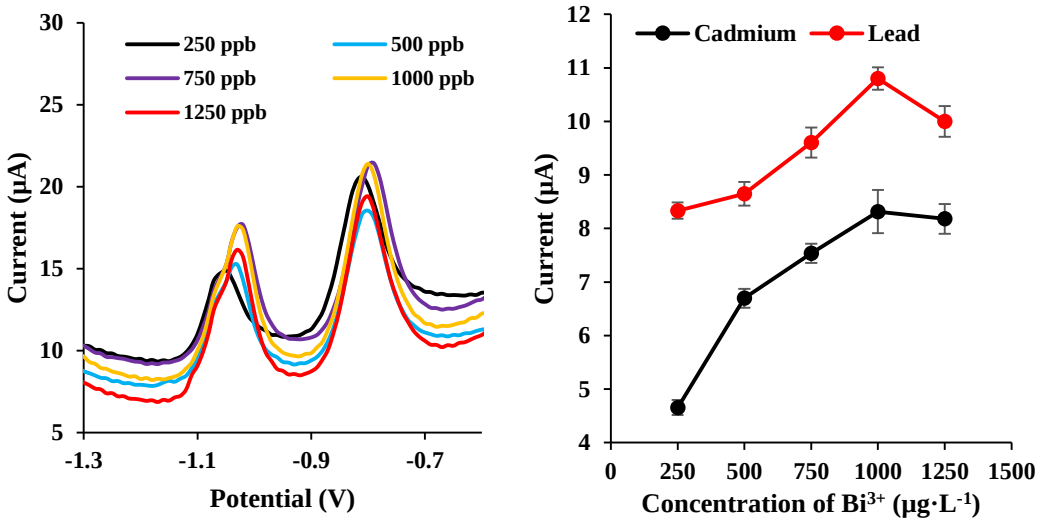

Figure 4.12 Effect of Bi^{3+} concentration on stripping peak of 50 µg·L^{-1} Cd^{2+} and Pb^{2+} with different concentration of Bi^{3+} in 0.1 M acetate buffer solution (pH 4.5). The error bars correspond to the standard deviation obtained from 3 measurement (n=3).

4.3.3.6 Effect of potential amplitude

The different potential amplitudes of 20, 40, 60 and 80 mV were used for studying an effect of potential amplitude on the electrochemical sensitivity of the system for the simultaneous determination of 50 µg·L^{-1} of Cd^{2+} and Pb^{2+} in the presence of 1000 µg·L^{-1} of Bi^{3+} while the results of ASV were shown in Figure 4.13 (left). The anodic current response obtained from ASV was plotted in the line graph as shown in Figure 4.13 (right). The results showed that, at the highest potential amplitude, it provides the highest current response for both Cd^{2+} and Pb^{2+}. However, the maximum value of potential amplitude was limited at 80 mV. Thus, a maximum potential amplitude of 80 mV was used as an optimum value for further experiments.

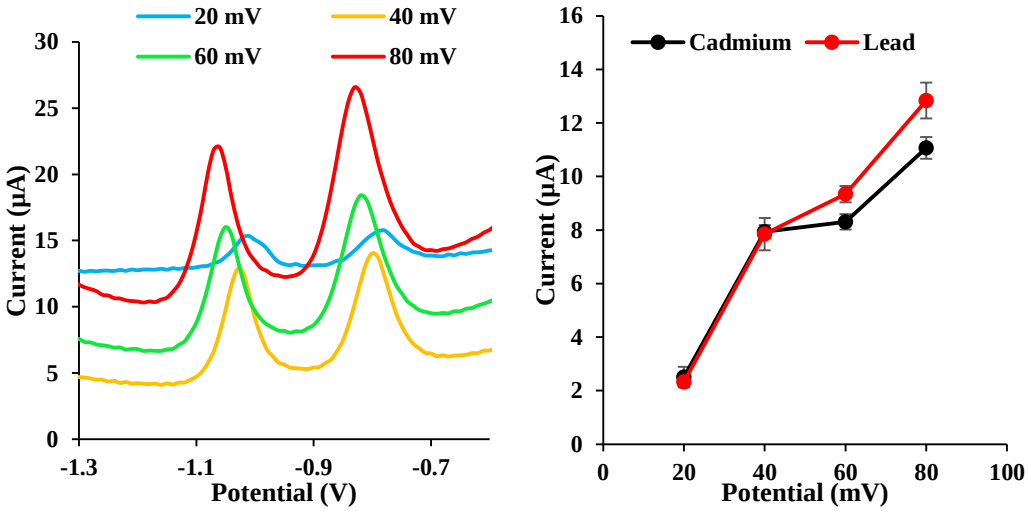

Figure 4.13 Effect of amplitude on stripping peak of 50 µg·L^{-1} of Cd^{2+} and Pb^{2+} in 0.1 M acetate buffer solution (pH 4.5). The error bars correspond to the standard deviation obtained from 3 measurement (n=3).

4.3.3.7 Effect of step potential

An influence of step potential was investigated for the simultaneous determination of 50 µg·L^{-1} of Cd^{2+} and Pb^{2+} with Bi^{3+} 1000 µg·L^{-1}. The different step potentials of 5, 10, 15 and 20 mV were studied. The results obtained from ASV were shown in Figure 4.14 (left) and the line graph was plotted in Figure 4.14 (right). The results showed that the current response of both Cd^{2+} and Pb^{2+} increase with increasing of the step potential. However, at the highest step potential, it provides the broad peak. So, the peak of Cd^{2+} was overlapped by the peak of Pb^{2+} leading to low electrochemical sensitivity. To solve this problem, a step potential of 15 mV was chosen and used as an optimum value for all further experiments.

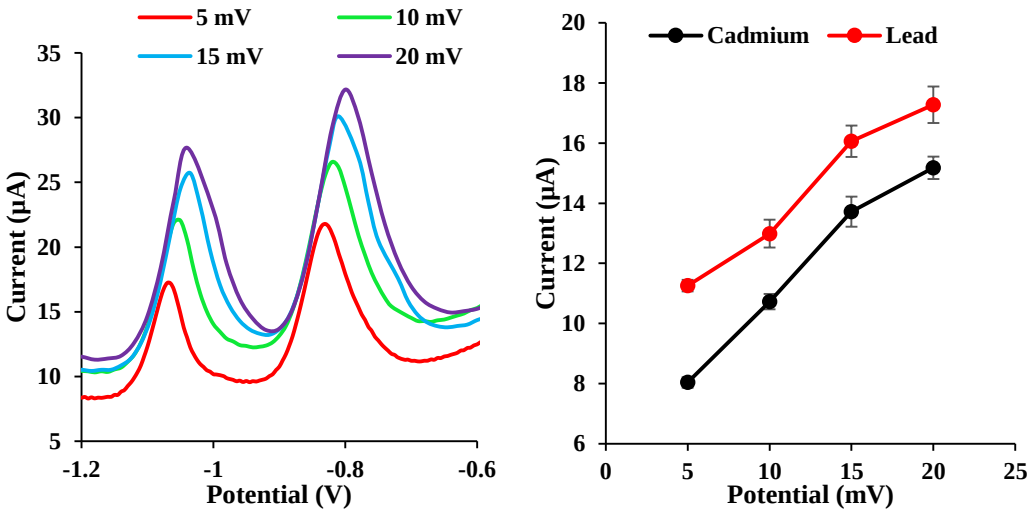

Figure 4.14 Effect of step potential on stripping peak of 50 µg·L^{-1} of Cd^{2+} and Pb^{2+} in 0.1 M acetate buffer solution (pH 4.5). The error bars correspond to the standard deviation obtained from 3 measurement (n=3).

4.3.3 The analytical sensitivity of electrode

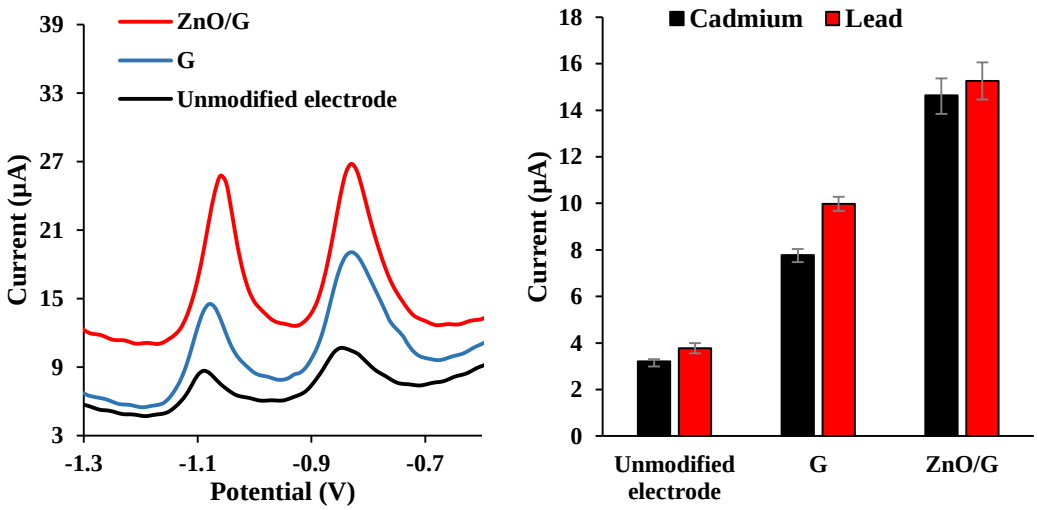

Figure 4.15 Anodic stripping voltammograms of ZnO/G modified electrode (red line), G modified electrode (blue line) and unmodified electrode (black line) on simultaneous detection of Cd^{2+} and Pb^{2+} at 50 µg·L^{-1} in 0.1 M acetate buffer pH 4.5 (A). The bar graph showing peak current obtained from ASV using ZnO/G modified electrode, G modified electrode and unmodified electrode. The error bars correspond to the standard deviation obtained from 3 measurement (n=3).

The analytical sensitivity of three electrodes including unmodified electrode, G modified electrode and ZnO/G modified electrode were studied by using ASV and measured the current response signal. The anodic stripping voltammograms of simultaneous determination of Cd^{2+} and Pb^{2+} measured on the ZnO/G modified electrode (red line), G modified electrode (blue line) and unmodified electrode (black line) with optimized conditions were shown in Figure 4.15 (left). The anodic peak potentials of Cd^{2+} and Pb^{2+} were measured at -1.1 and -0.8V, respectively. From the results, the anodic peak current response of ZnO/G modified electrode was approximately 1.5 and 4 folds higher than the current response obtained on G modified electrode and unmodified electrode for both Cd^{2+} and Pb^{2+} indicating that there is synergistic effect between ZnO and G, which can enhance the electrochemical sensitivity for the simultaneous determination of Cd^{2+} and Pb^{2+}.

4.3.4 Analytical performance of ZnO/G modified electrode

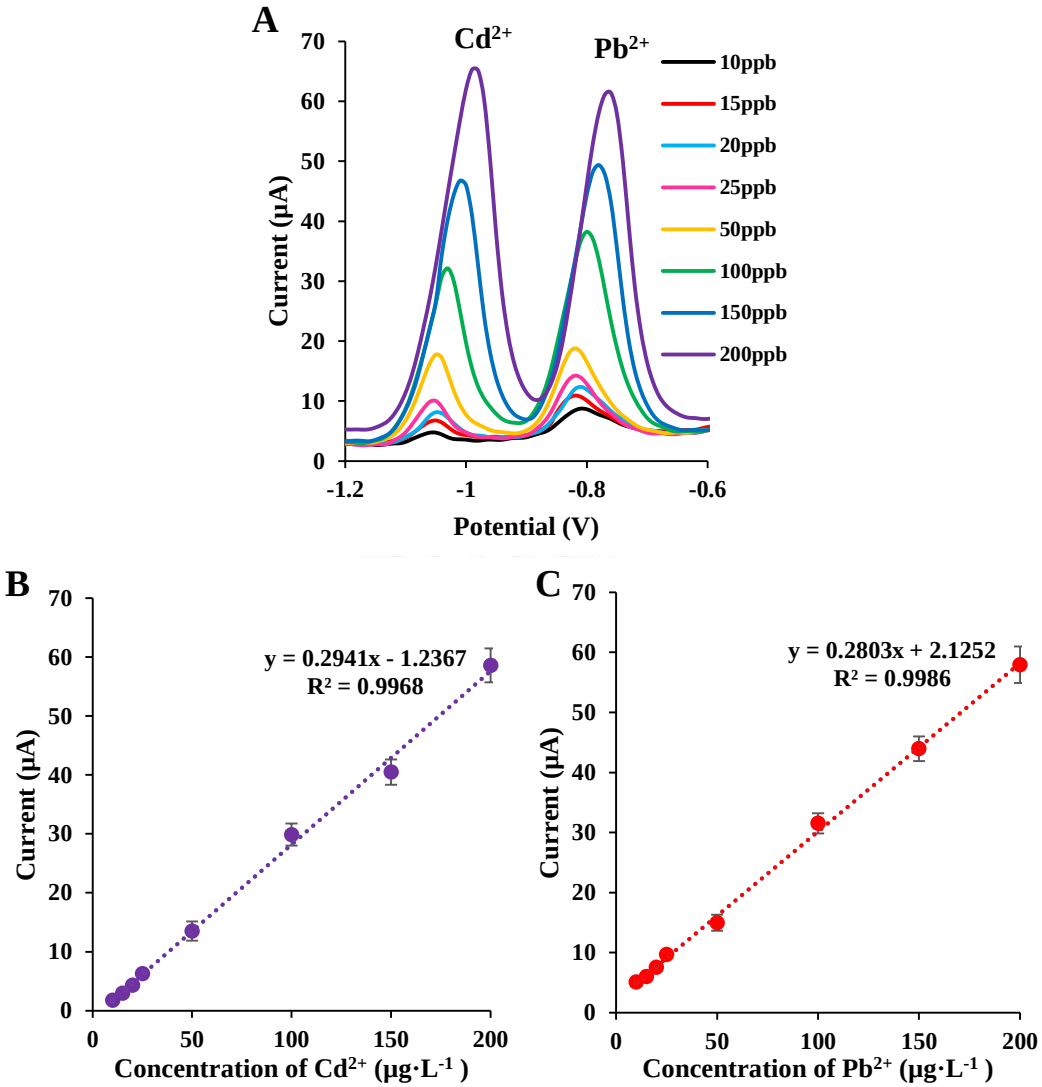

Figure 4.16 Anodic stripping voltammograms of $Cd^{2+}$and Pb^{2+} in various concentration range of 10-200 µg·L^{-1} (A), the calibration plot of Cd^{2+} concentration versus the current response (B) and the calibration plot of Pb^{2+} versus the current response (C). The error bars correspond to the standard deviation obtained from 3 measurement (n=3).

Under the optimized conditions, the analytical performances of ZnO/G nanocomposite modified electrode for the simultaneous determination of Cd^{2+} and Pb^{2+} were evaluated (Figure 4.16). The peaks obtained from ASV with different concentration of Cd^{2+} and Pb^{2+} were shown in Figure 4.16A, the linear ranges for both Cd^{2+} and Pb^{2+} were found in the range from 10 to 200 µg·L^{-1}. The calibration plots of

various concentrations of Cd^{2+} and Pb^{2+} versus the anodic current responses were shown in Figure 4.16B and 4.16C, respectively. The correlation coefficient values (R^2) were found to be 0.9968 and 0.9986 for Cd^{2+} and Pb^{2+}, respectively. The limits of detection (LOD) of Cd^{2+} and Pb^{2+} were calculated by LOD = $3S.D._b/M$ (where $S.D._b$ is the standard deviation from the blank measurement, and M is a slope from the calibration curve of the standard). The LODs were found to be 0.6 $\mu g \cdot L^{-1}$ for Cd^{2+} and 0.8 $\mu g \cdot L^{-1}$ for $Pb^{2+,}$ respectively. Moreover, the analytical performances of proposed electrode were compared with other electrodes for the simultaneous determination of Cd^{2+} and Pb^{2+} as seen in Table 4.1. It was indicated that, our developed system provides comparable limit of detection and linear range for simultaneous determination of Cd^{2+} and Pb^{2+}. Moreover, this system is easy to produce and also inexpensive. Therefore, this proposed system might be an alternative device for the simultaneous determination of Cd^{2+} and Pb^{2+}.

Table 4.1 Comparison of proposed electrode and other electrode in the determination of Cd^{2+} and Pb^{2+}.

Electrode	LOD ($\mu g \cdot L^{-1}$)		Linear range ($\mu g \cdot L^{-1}$)		Ref.
	Cd^{2+}	Pb^{2+}	Cd^{2+}	Pb^{2+}	
G-MWCNTs/GCE	0.1	0.2	0.5-30	0.5-30	[54]
Bi_2O_3/PSS/CnP/SPCE	0.1	0.3	5-40	5-40	[55]
NH_2-MCM-41-nafion/GCE	1.0	0.2	50-450	0.5-250	[56]
TiO_2/ZrO_2/CPE	0.77	0.48	1-200	1-200	[57]
ERGNO film/SPCE	0.50	0.80	1-60	1-60	[58]
Bi-CNT/SPCE	1.3	0.7	2-100	2-100	[59]
G/PANI/PS nanoporous fiber/SPCE	4.43	3.30	10-500	10-500	[3]
ZnO-nanorods/G/SPCE	0.6	0.8	10-200	10-200	This work

4.3.5 Interference study

In general, there are many ions presenting in water sample, including Na^{+}, K^{+}, Ca^{2+}, Mg^{2+}, Ba^{2+}, Cu^{2+}, Co^{2+}, Ni^{2+}, Zn^{2+}, Mn^{2+}, Fe^{3+}, Cl^{-}, SO_4^{2-} and NO_3^{-} which might interfere the current response of target heavy metals in ASV. Thus, an effect of other ions on the simultaneous determination of Cd^{2+} and Pb^{2+} was investigated and reported as a tolerance ratio (±5% signal response change was acceptable). From the results, a 1000-fold mass ratio of Na^{+}, K^{+}, Ca^{2+}, Mg^{2+}, Ba^{2+}, Cl^{-}, SO_4^{2-}, a 300-fold mass ratio of Co^{2+}, Fe^{3+} and NO_3^{-}, a 200-fold mass ratio of Mn^{2+}, a 10-fold mass ratio of Zn^{2+} and Ni^{2+} and a 5-fold mass ratio of Cu^{2+} do not interfere in the simultaneous determination of Cd^{2+} and Pb^{2+} at 50 $\mu g \cdot L^{-1}$. However, in case of high level of Zn^{2+}, Cu^{2+} and Ni^{2+}, these ions can potentially interfere the target analytes leading to low current response signal of this system.

4.3.6 Real sample analyses

Under the optimum conditions, ZnO/G modified electrode was applied for the simultaneous detection of Cd^{2+} and Pb^{2+} in industrial wastewater samples. To validate the results obtained from our system, a standard method (ICP-OES) was used and the data were shown in Table 4.2. The results obtained from our method corresponded very well with the results obtained from ICP-OES method. The percentage recoveries were found in a range from 98.04 to 109.00 for Cd^{2+} and 94.3 to 104.11 for Pb^{2+}, indicating that this ZnO/G modified electrode might be useful as an alternative tool for the simultaneous detection of Cd^{2+} and Pb^{2+} in wastewater samples.

Table 4.2 Determination of Cd^{2+} and Pb^{2+} in wastewater samples using proposed method compared with standard method (ICP-OES).

Sample	Add ($\mu g \cdot L^{-1}$)	Cadmium		Recovery (%)
	Cd^{2+}	Found ± SD ($\mu g \cdot L^{-1}$)	ICP-OES ± SD ($\mu g \cdot L^{-1}$)	Cd^{2+}
Wastewater-1	0	2.07 ± 0.20	1.20 ± 0.04	-
	10	12.77 ± 1.00	11.13 ± 0.06	106.97 ± 8.02
	50	55.41 ± 2.85	54.04 ± 0.12	106.68 ± 5.31
	100	110.29 ± 2.79	105.80 ± 0.35	108.22 ± 2.94

Sample	Add ($\mu g \cdot L^{-1}$)	Lead		Recovery (%)
	Pb^{2+}	Found ± SD ($\mu g \cdot L^{-1}$)	ICP-OES ± SD ($\mu g \cdot L^{-1}$)	Pb^{2+}
Wastewater-1	0	13.27 ± 1.60	14.2 ± 0.23	-
	10	22.7 ± 1.11	24.5 ± 0.22	94.3 ± 5.65
	50	65.32 ± 2.63	64.8 ± 0.59	104.11 ± 7.00
	100	112.69 ± 2.93	109.4 ± 1.23	100.25 ± 3.39

Sample	Add ($\mu g \cdot L^{-1}$)	Cadmium		Recovery (%)
	Cd^{2+}	Found ± SD ($\mu g \cdot L^{-1}$)	ICP-OES ± SD ($\mu g \cdot L^{-1}$)	Cd^{2+}
Wastewater-2	0	1.67 ± 0.38	2.12 ± 0.07	-
	10	11.67 ± 0.66	9.76 ± 0.05	99.67 ± 8.25
	50	50.72 ± 3.04	51.31 ± 0.12	98.04 ± 6.41
	100	101.62 ± 2.10	102.72 ± 0.33	99.92 ± 2.07

Sample	Add ($\mu g \cdot L^{-1}$)	Lead		Recovery (%)
	Pb^{2+}	Found ± SD ($\mu g \cdot L^{-1}$)	ICP-OES ± SD ($\mu g \cdot L^{-1}$)	Pb^{2+}
Wastewater-2	0	24.81 ± 0.76	17.20 ± 0.08	-
	10	34.40 ± 0.74	36.84 ± 0.05	95.93 ± 8.41
	50	73.09 ± 2.43	72.01 ± 0.13	96.55 ± 4.38
	100	122.25 ± 2.06	125.10 ± 1.11	97.44 ± 2.81

Sample	Add ($\mu g \cdot L^{-1}$)	Cadmium		Recovery (%)
	Cd^{2+}	Found ± SD ($\mu g \cdot L^{-1}$)	ICP-OES ± SD ($\mu g \cdot L^{-1}$)	Cd^{2+}
Wastewater-3	0	1.29 ± 0.26	0.77 ± 0.08	-
	10	12.19 ± 0.39	11.65 ± 0.12	109.00 ± 5.77
	50	52.22 ± 1.38	52.01 ± 0.26	101.86 ± 2.25
	100	107.87 ± 3.89	107.04 ± 0.32	106.58 ± 3.68

Sample	Add ($\mu g \cdot L^{-1}$)	Lead		Recovery (%)
	Pb^{2+}	Found ± SD ($\mu g \cdot L^{-1}$)	ICP-OES ± SD ($\mu g \cdot L^{-1}$)	Pb^{2+}
Wastewater-3	0	39.92 ± 1.46	42.76 ± 0.12	-
	10	49.51 ± 2.11	48.53 ± 0.04	103.4 ± 7.81
	50	90.17 ± 2.34	81.29 ± 0.12	101.98 ± 2.30
	100	141.44 ± 3.45	142.87 ± 1.15	102.26 ± 2.87

CHAPTER V
CONCLUSIONS

5.1 Conclusions

In this study, the ZnO nanorods were prepared by zinc acetate via thermal decomposition method. Then, the as prapared ZnO nanorods were used to synthesize ZnO/G nanocomposites through a colloidal coagulation effect. The obtained ZnO/G nanocomposites were originally applied to modify the working electrode surface for the simultaneous determination of Cd^{2+} and Pb^{2+} by using ASV. Under the optimum conditions, the anodic current responses of Cd^{2+} and Pb^{2+} obtained from ZnO/G modified SPCE were approximately 4 folds higher than the anodic current response obtained from an unmodified SPCE, verifying the improved electrochemical sensitivity in the determination of Cd^{2+} and Pb^{2+}. The linear ranges were found to be 10-200 $\mu g \cdot L^{-1}$ for both Cd^{2+} and Pb^{2+}. The detection limits of Cd^{2+} and Pb^{2+} were 0.6 and 0.8 $\mu g \cdot L^{-1}$, respectively. Furthermore, our system was successfully applied for the simultaneous determination of Cd^{2+} and Pb^{2+} in wastewater samples. The results were corresponded well with the ICP-OES results with the percentage recoveries in the ranges of 98-109% and 94-104% for Cd^{2+} and Pb^{2+}, respectively.

5.2 Suggestion for future work

A novel electrode system based on ZnO/G modified SPCE developed in this work might be used as an alternative sensing tool for various applications, such as medical diagnosis, food inspection and environment monitoring.

In a concept of this work, ZnO nanorods were intercalated between G sheets for an improvement of G properties by their synergistic effects. Moreover, the re-stacking of G sheets can be prevented by insertion of ZnO nanorods. However, ZnO is a semi-conductor, the conductivity performance is not sufficient. To increase the conductivity, using G with other highly conductive nanomaterials, such as gold nanorods and platinum nanorods might be an alternative way to further improve the sensor sensitivity.

REFERENCES

[1] Yukird, J., T. Wongtangprasert, R. Rangkupan, O. Chailapakul, T. Pisitkun and N. Rodthongkum, Label-free immunosensor based on graphene/polyaniline nanocomposite for neutrophil gelatinase-associated lipocalin detection, Biosensors and Bioelectronics 87 (2017) 249-255.

[2] Shrestha, S., R.J. Mascarenhas, O.J. D'Souza, A.K. Satpati, Z. Mekhalif, A. Dhason and P. Martis, Amperometric sensor based on multi-walled carbon nanotube and poly (Bromocresol purple) modified carbon paste electrode for the sensitive determination of L-tyrosine in food and biological samples, Journal of Electroanalytical Chemistry 778 (2016) 32-40.

[3] Promphet, N., P. Rattanarat, R. Rangkupan, O. Chailapakul and N. Rodthongkum, An electrochemical sensor based on graphene/polyaniline/polystyrene nanoporous fibers modified electrode for simultaneous determination of lead and cadmium, Sensors and Actuators B: Chemical 207, Part A (2015) 526-534.

[4] Saengsookwaow, C., R. Rangkupan, O. Chailapakul and N. Rodthongkum, Nitrogen-doped graphene–polyvinylpyrrolidone/gold nanoparticles modified electrode as a novel hydrazine sensor, Sensors and Actuators B: Chemical 227 (2016) 524-532.

[5] Rodthongkum, N., N. Ruecha, R. Rangkupan, R.W. Vachet and O. Chailapakul, Graphene-loaded nanofiber-modified electrodes for the ultrasensitive determination of dopamine, Analytica Chimica Acta 804 (2013) 84-91.

[6] Lee, P.M., Z. Wang, X. Liu, Z. Chen and E. Liu, Glassy carbon electrode modified by graphene–gold nanocomposite coating for detection of trace lead ions in acetate buffer solution, Thin Solid Films 584 (2015) 85-89.

[7] Cembrero, J., A. Pruna, D. Pullini and D. Busquets-Mataix, Effect of combined chemical and electrochemical reduction of graphene oxide on morphology and structure of electrodeposited ZnO, Ceramics International 407, Part B (2014) 10351-10357.

[8] Zhang, B.T., X. Zheng, H.F. Li and J.M. Lin, Application of carbon-based nanomaterials in sample preparation: a review, Analytica Chimica Acta 784 (2013) 1-17.

[9] Lonkar, S.P., Y.S. Deshmukh and A.A. Abdala, Recent advances in chemical modifications of graphene, Nano Research 84 (2014) 1039-1074.

[10] Yang, Y., C. Han, B. Jiang, J. Iocozzia, C. He, D. Shi, T. Jiang and Z. Lin, Graphene-based materials with tailored nanostructures for energy conversion and storage, Materials Science and Engineering: R: Reports 102 (2016) 1-72.

[11] Liu, J., L. Cui and D. Losic, Graphene and graphene oxide as new nanocarriers for drug delivery applications, Acta Biomater 912 (2013) 9243-57.

[12] Huang, H.-P. and J.-J. Zhu, Preparation of Novel Carbon-based Nanomaterial of Graphene and Its Applications Electrochemistry, Chinese Journal of Analytical Chemistry 397 (2011) 963-971.

[13] Pumera, M., Electrochemistry of graphene, graphene oxide and other graphenoids: Review, Electrochemistry Communications 36 (2013) 14-18.

[14] Ji, X., Y. Xu, W. Zhang, L. Cui and J. Liu, Review of functionalization, structure and properties of graphene/polymer composite fibers, Composites Part A: Applied Science and Manufacturing 87 (2016) 29-45.

[15] Pruna, A., Q. Shao, M. Kamruzzaman, J.A. Zapien and A. Ruotolo, Enhanced electrochemical performance of ZnO nanorod core/polypyrrole shell arrays by graphene oxide, Electrochimica Acta 187 (2016) 517-524.

[16] Zhihua, L., Z. Xucheng, W. Kun, Z. Xiaobo, S. Jiyong, H. Xiaowei and M. Holmes, A novel sensor for determination of dopamine in meat based on ZnO-decorated reduced graphene oxide composites, Innovative Food Science & Emerging Technologies 31 (2015) 196-203.

[17] Hou, X., F. Zhou and W. Liu, A facile low-cost synthesis of ZnO nanorods via a solid-state reaction at low temperature, Materials Letters 6029–30 (2006) 3786-3788.

[18] Jayaraman, S., P. Suresh Kumar, D. Mangalaraj, R. Dharmarajan, S. Ramakrishna and M. P Srinivasan, Gold nanoparticle immobilization on ZnO nanorods via bi-

functional monolayers: A facile method to tune interface properties, Surface Science 641 (2015) 23-29.

[19] Deng, J., M. Wang, P. Zhang and W. Ye, Preparing ZnO nanowires in mesoporous TiO2 photoanode by an in-situ hydrothermal growth for enhanced light-trapping in quantum dots-sensitized solar cells, Electrochimica Acta 200 (2016) 12-20.

[20] Qu, X., S. Lü, J. Wang, Z. Li and H. Xue, Preparation and optical property of porous ZnO nanobelts, Materials Science in Semiconductor Processing 153 (2012) 244-250.

[21] Chen, Y.-H., Y.-M. Shen, S.-C. Wang and J.-L. Huang, Fabrication of one-dimensional ZnO nanotube and nanowire arrays with an anodic alumina oxide template via electrochemical deposition, Thin Solid Films 570, Part B (2014) 303-309.

[22] Quartarone, E., V. Dall'Asta, A. Resmini, C. Tealdi, I.G. Tredici, U.A. Tamburini and P. Mustarelli, Graphite-coated ZnO nanosheets as high-capacity, highly stable, and binder-free anodes for lithium-ion batteries, Journal of Power Sources 320 (2016) 314-321.

[23] Kang, W., X. Jimeng and W. Xitao, The effects of ZnO morphology on photocatalytic efficiency of ZnO/RGO nanocomposites, Applied Surface Science 360, Part A (2016) 270-275.

[24] Peng, Y., J. Ji and D. Chen, Ultrasound assisted synthesis of ZnO/reduced graphene oxide composites with enhanced photocatalytic activity and anti-photocorrosion, Applied Surface Science 356 (2015) 762-768.

[25] Nipane, S.V., P.V. Korake and G.S. Gokavi, Graphene-zinc oxide nanorod nanocomposite as photocatalyst for enhanced degradation of dyes under UV light irradiation, Ceramics International 413, Part B (2015) 4549-4557.

[26] Low, S.S., M.T.T. Tan, H.-S. Loh, P.S. Khiew and W.S. Chiu, Facile hydrothermal growth graphene/ZnO nanocomposite for development of enhanced biosensor, Analytica Chimica Acta 903 (2016) 131-141.

[27] Hwa, K.-Y. and B. Subramani, Synthesis of zinc oxide nanoparticles on graphene–carbon nanotube hybrid for glucose biosensor applications, Biosensors and Bioelectronics 62 (2014) 127-133.

[28] Zhang, X., Y.-C. Zhang and L.-X. Ma, One-pot facile fabrication of graphene-zinc oxide composite and its enhanced sensitivity for simultaneous electrochemical detection of ascorbic acid, dopamine and uric acid, Sensors and Actuators B: Chemical 227 (2016) 488-496.

[29] Afkhami, A., H. Ghaedi, T. Madrakian and M. Rezaeivala, Highly sensitive simultaneous electrochemical determination of trace amounts of Pb(II) and Cd(II) using a carbon paste electrode modified with multi-walled carbon nanotubes and a newly synthesized Schiff base, Electrochimica Acta 89 (2013) 377-386.

[30] Magos, L., T. C. Hutchinson and K. M. Meema (Editors). Lead, Mercury, Cadmium and Arsenic in the Environment. Scope 31. John Wiley & Sons, Chichester, 1987; 360 pp, £48.00, Journal of Applied Toxicology 82 (1988) 150-151.

[31] Bagheri, H., A. Afkhami, M. Saber-Tehrani and H. Khoshsafar, Preparation and characterization of magnetic nanocomposite of Schiff base/silica/magnetite as a preconcentration phase for the trace determination of heavy metal ions in water, food and biological samples using atomic absorption spectrometry, Talanta 97 (2012) 87-95.

[32] Ammann, A.A., Speciation of heavy metals in environmental water by ion chromatography coupled to ICP–MS, Analytical and Bioanalytical Chemistry 3723 (2002) 448-452.

[33] Silva, E.L., P.d.S. Roldan and M.F. Giné, Simultaneous preconcentration of copper, zinc, cadmium, and nickel in water samples by cloud point extraction using 4-(2-pyridylazo)-resorcinol and their determination by inductively coupled plasma optic emission spectrometry, Journal of Hazardous Materials 1711–3 (2009) 1133-1138.

[34] Aragay, G. and A. Merkoçi, Nanomaterials application in electrochemical detection of heavy metals, Electrochimica Acta 84 (2012) 49-61.

[35] Ouyang, R., Z. Zhu, C.E. Tatum, J.Q. Chambers and Z.-L. Xue, Simultaneous stripping detection of Zn(II), Cd(II) and Pb(II) using a bimetallic Hg–Bi/single-walled carbon nanotubes composite electrode, Journal of Electroanalytical Chemistry 6561–2 (2011) 78-84.

[36] Mussini, P.R., Analytical Electrochemistry, 3rd ed., J. Wang. Wiley–VCH, New York (2006), Electrochimica Acta 538 (2008) 3446-3448.

[37] Bard, A.J. and L.R. Faulkner, Fundamentals and Applications. 2nd ed. 2001, New York, USA: Jonh Wiley & Sons.

[38] Mohamed, H.M., Screen-printed disposable electrodes: Pharmaceutical applications and recent developments, TrAC Trends in Analytical Chemistry 82 (2016) 1-11.

[39] Tashkhourian, J., B. Hemmateenejad, H. Beigizadeh, M. Hosseini-Sarvari and Z. Razmi, ZnO nanoparticles and multiwalled carbon nanotubes modified carbon paste electrode for determination of naproxen using electrochemical techniques, Journal of Electroanalytical Chemistry 714–715 (2014) 103-108.

[40] Zhang, B.-T., X. Zheng, H.-F. Li and J.-M. Lin, Application of carbon-based nanomaterials in sample preparation: A review, Analytica Chimica Acta 7840 (2013) 1-17.

[41] Wonsawat, W., S. Chuanuwatanakul, W. Dungchai, E. Punrat, S. Motomizu and O. Chailapakul, Graphene-carbon paste electrode for cadmium and lead ion monitoring in a flow-based system, Talanta 100 (2012) 282-289.

[42] Liu, J., G. Zhu, M. Chen, X. Ma and J. Yang, Fabrication of electrospun ZnO nanofiber-modified electrode for the determination of trace Cd(II), Sensors and Actuators B: Chemical 234 (2016) 84-91.

[43] Lee, S., J. Oh, D. Kim and Y. Piao, A sensitive electrochemical sensor using an iron oxide/graphene composite for the simultaneous detection of heavy metal ions, Talanta 160 (2016) 528-36.

[44] Wei, Y., C. Gao, F.-L. Meng, H.-H. Li, L. Wang, J.-H. Liu and X.-J. Huang, SnO2/Reduced Graphene Oxide Nanocomposite for the Simultaneous Electrochemical Detection of Cadmium(II), Lead(II), Copper(II), and Mercury(II): An Interesting Favorable Mutual Interference, The Journal of Physical Chemistry C 1161 (2012) 1034-1041.

[45] Lin, H., X. Li, X. He and J. Zhao, Application of a novel 3D nano-network structure for Ag-modified TiO2 film electrode with enhanced electrochemical performance, Electrochimica Acta 173 (2015) 242-251.

[46] Arabali, V., M. Ebrahimi and H. Karimi-Maleh, Highly sensitive determination of promazine in pharmaceutical and biological samples using a ZnO nanoparticle-modified ionic liquid carbon paste electrode, Chinese Chemical Letters 275 (2016) 779-782.

[47] Lu, Y.-Y., M.-N. Chen, Y.-L. Gao, J.-M. Yang, X.-Y. Ma and J.-Y. Liu, Preparation of Zinc Oxide-Graphene Composite Modified Electrodes for Detection of Trace Pb(II), Chinese Journal of Analytical Chemistry 439 (2015) 1395-1401.

[48] Florence, T.M., Anodic stripping voltammetry with a glassy carbon electrode mercury-plated in situ, Journal of Electroanalytical Chemistry and Interfacial Electrochemistry 272 (1970) 273-281.

[49] Lee, S., S.-K. Park, E. Choi and Y. Piao, Voltammetric determination of trace heavy metals using an electrochemically deposited graphene/bismuth nanocomposite film-modified glassy carbon electrode, Journal of Electroanalytical Chemistry 766 (2016) 120-127.

[50] Serrano, N., J.M. Díaz-Cruz, C. Ariño and M. Esteban, Ex situ Deposited Bismuth Film on Screen-Printed Carbon Electrode: A Disposable Device for Stripping Voltammetry of Heavy Metal Ions, Electroanalysis 2213 (2010) 1460-1467.

[51] Qin, J., X. Zhang, Y. Xue, N. Kittiwattanothai, P. Kongsittikul, N. Rodthongkum, S. Limpanart, M. Ma and R. Liu, A facile synthesis of nanorods of ZnO/graphene oxide composites with enhanced photocatalytic activity, Applied Surface Science 321 (2014) 226-232.

[52] Molefe, F.V., L.F. Koao, B.F. Dejene and H.C. Swart, Phase formation of hexagonal wurtzite ZnO through decomposition of Zn(OH)2 at various growth temperatures using CBD method, Optical Materials 46 (2015) 292-298.

[53] Chen, C., X. Niu, Y. Chai, H. Zhao and M. Lan, Bismuth-based porous screen-printed carbon electrode with enhanced sensitivity for trace heavy metal detection by stripping voltammetry, Sensors and Actuators B: Chemical 178 (2013) 339-342.

[54] Huang, H., T. Chen, X. Liu and H. Ma, Ultrasensitive and simultaneous detection of heavy metal ions based on three-dimensional graphene-carbon nanotubes hybrid electrode materials, Analytica Chimica Acta 852 (2014) 45-54.

[55] María-Hormigos, R., M.J. Gismera, J.R. Procopio and M.T. Sevilla, Disposable screen-printed electrode modified with bismuth–PSS composites as high sensitive sensor for cadmium and lead determination, Journal of Electroanalytical Chemistry 767 (2016) 114-122.

[56] Dai, X., F. Qiu, X. Zhou, Y. Long, W. Li and Y. Tu, Amino-functionalized MCM-41 for the simultaneous electrochemical determination of trace lead and cadmium, Electrochimica Acta 144 (2014) 161-167.

[57] Nguyen, P.K.Q. and S.K. Lunsford, Square wave anodic stripping voltammetric analysis of lead and cadmium utilizing titanium dioxide/zirconium dioxide carbon paste composite electrode, Journal of Electroanalytical Chemistry 711 (2013) 45-52.

[58] Ping, J., Y. Wang, J. Wu and Y. Ying, Development of an electrochemically reduced graphene oxide modified disposable bismuth film electrode and its application for stripping analysis of heavy metals in milk, Food Chemistry 151 (2014) 65-71.

[59] Hwang, G.H., W.K. Han, J.S. Park and S.G. Kang, Determination of trace metals by anodic stripping voltammetry using a bismuth-modified carbon nanotube electrode, Talanta 762 (2008) 301-308.

APPENDIX

VITA

Pongsakorn Kongsittikul was born on October 18, 1991 in Bangkok, Thailand. He received his Bachelor Degree of Engineering, majoring in Petrochemicals and Polymeric Materials from Silpakorn University, Nakhon Pathom, Thailand (2009-2013). He expect graduated his Master Degree of Science, majoring in Petrochemistry and Polymer Science from Chulalongkorn University, Bangkok, Thailand in 2016.

Oral presentation

Pongsakorn Kongsittikul, Kanokwan Saengkiettiyut, Jiaqian Qin, Nadnudda Rodthongkum, Orawon Chailapakul, “Zinc oxide/graphene nanocomposite as a novel electrode for heavy metal sensing” Pure and Applied chemistry International Conference 2016 (PACCON2016), Febuary 9-11, 2016, Bangkok, Thailand.

Proceeding

Pongsakorn Kongsittikul, Kanokwan Saengkiettiyut, Jiaqian Qin, Nadnudda Rodthongkum, Orawon Chailapakul, “Zinc oxide/graphene nancomposite as a novel electrode for heavy metal sensing” Proceeding of Pure and Applied chemistry International Conference 2016.